

OPTIMUM ENERGY EFFICIENCY IN MASSIVE MIMO SYSTEM



By

Saira Jabeen

MSEE-19

Submitted to the Faculty of Department of Electrical Engineering
Military College of Signals, Rawalpindi
National University of Sciences and Technology, in partial fulfillment
for the requirements of MS Degree in Electrical Engineering (Telecommunication)

January 2016

SUPERVISOR CERTIFICATE

It is certified that the Final Copy of Thesis has been evaluated by me, found as per specified format and error free.

Dated _____

(Col Dr Imran Rashid)

ABSTRACT

Ever growing demand for new services and ubiquitous connectivity increases the energy consumption. Energy efficient communication system cover a given area with maximal energy efficiency (bit/joule) using massive MIMO setup. Energy efficiency of a large MIMO system is closely related to its power consumption. It depends on various design parameters; in particular, the network architecture, the user terminals, spectral efficiency, the average radiated signal power per user, the number of antennas that are deployed at the access points and circuit power consumption. In BS large number of antennas serve comparatively small number of user to fulfil the Massive multiple-input multiple-output (MIMO) requirements as a result more energy and spectral efficiency is achieved as compared to traditional MIMO technology. Using different processing schemes at the base station a new detailed power consumption model is propose that shows how different parameters like active users, optimal number of antennas at base station and transmit power affect the energy efficiency. Numerical and analytical results show that using massive MIMO setup where large number of BS antennas are deployed to serve less number of users, maximal energy efficiency is obtained. Interestingly, increasing number of antennas at base station also increases the total circuit power consumption from analog devices but energy efficiency is less sensitive to power consumption in Massive MIMO setup. So energy efficiency after reaching its maximum value maintain its position.

Dedicated to,

My beloved Parents,

Who taught me how to read and learn and who always encouraged higher education,
for their prayers, love and motivation and sacrifices all along.

My sisters for their love, support and patience during all the phases of my MS

ACKNOWLEDGMENTS

I would like to express my deepest gratitude to my supervisor, Col Dr. Imran Rashid, without whose guidance and support this dissertation would not have been possible. During my MS studies, his insightful guidance and unwavering support have always been inspiring me for conducting cutting-edge research and lead me through the difficult times. I am also indebted to my co-Supervisor and my committee members Lt Col Faisal Akram, Col Dr. Abdul Rauf and Dr. Imran for their help and support. Finally, my parents have been a constant source of inspiration for me. They have always been with me with their prayers and well wishes.

TABLE OF CONTENTS

<i>Chapter 1</i>	1
Introduction	1
1.1 How Mobile Data Traffic effects Energy Efficiency?	2
1.2 Why Energy Efficiency?.....	3
1.2.1 Solutions Available.....	5
1.2.2 Reason/ Justification for the Selection of the Topic	6
1.2.3 Proposed Solution	7
1.3 Methodology	7
1.4 Organization.....	8
1.5 Notation.....	8
<i>Chapter 02</i>	9
MIMO, Multi User MIMO and Massive MIMO	9
2.1 MIMO - An overview	9
2.2 Spatial Multiplexing Gain.....	10
2.2.1 Spatial Multiplexing Receivers.....	11
2.2.2 Successive Interference Cancellation	12
2.3 Spatial Diversity.....	12
2.3.1 Transmit Diversity	13
2.3.2 Receive Diversity.....	13
2.4 Massive MIMO	15

2.5	Summary	18
Chapter 03		19
Energy Efficiency		19
3.1	Introduction to EE (energy efficiency)	19
3.2	Circuit power consumption model	22
3.3	Summary	23
Chapter 4		24
Optimum EE in Massive MIMO using MRT and ZF Precoding		24
4.1	Problem Formulation	24
4.2	EE Metrics	25
4.2.1	Linear Processing	26
4.3	EE Optimization with ZF processing	28
4.4	Simulation with ZF processing	30
4.4.1	ZF with Perfect CSI	30
4.4.2	ZF with Imperfect CSI	31
4.5	EE Optimization with MRT/MRC processing	31
4.6	Simulation with MRT/MRC processing	33
4.7	Optimal Number of Users	34
4.8	Optimal Number of BS Antennas	35
4.9	Optimal RF Power	35
4.10	EE Optimization with Multi-cell Scenario	36
Chapter 5		39

Optimum EE in Massive MIMO using MMSE Precoding	39
5.1 Problem Statement	39
5.2 Realistic Circuit Power Consumption Model	40
5.3 Energy Efficiency Optimization with MMSE Processing	44
5.4 Simulation with MMSE Processing.....	46
5.5 Comparison of MMSE with ZF and MRT Processing.....	48
Chapter 6	51
Conclusions and Future Work.....	51
6.1 Conclusion	51
6.2 Future Work	52
References.....	53

LIST OF FIGURES

FIGURE 1: MOBILE TRAFFIC FORECAST 2012-2017 WITH A COMPOUND ANNUAL GROWTH	3
FIGURE 2: MIMO SYSTEM FOR MULTIPLE TRANSMIT AND RECEIVE ANTENNAS	10
FIGURE 3: A SIMPLIFIED MASSIVE MIMO SYSTEM.....	18
FIGURE 4: CELLULAR NETWORK POWER CONSUMPTION AND CIRCUIT POWER CONSUMPTION AT BASE STATIONS	19
FIGURE 5: EE VERSUS SNR WITHOUT CONSIDERATION OF CIRCUIT POWER CONSUMPTION.....	21
FIGURE 6: EE VERSUS SNR WITH CONSIDERATION OF CIRCUIT POWER CONSUMPTION.	21
FIGURE 7: ILLUSTRATION OF THE TDD PROTOCOL.....	24
FIGURE 8: A GENERIC MU- MIMO SCENARIO.	25
FIGURE 9: ZF PROCESSING SINGLE CELL SCENARIO AND PERFECT CSI.....	30
FIGURE 10: ZF SINGLE CELL SCENARIO AND IMPERFECT CSI.....	31
FIGURE 11: MRT/MRC PROCESSING WITH SINGLE CELL SCENARIO AND PERFECT CSI.....	33
FIGURE 12: ENERGY EFFICIENCY (IN MBIT/JOULE) WITH ZF PROCESSING IN THE MULTI CELL.....	36
FIGURE 13: MAXIMAL EE IN THE MULTI-CELL SCENARIO FOR DIFFERENT NUMBER OF BS ANTENNAS AND DIFFERENT PILOT REUSE FACTORS.	37
FIGURE 14: TOTAL RF POWER AT THE EE-MAXIMIZING SOLUTION IN THE MULTI-CELL SCENARIO, FOR DIFFERENT NUMBER OF BS ANTENNAS. THE RADIATED POWER PER BS ANTENNA IS ALSO SHOWN.	37
FIGURE 15: AREA THROUGHPUT AT THE EE-MAXIMIZING SOLUTION IN THE MULTI-CELL SCENARIO, FOR DIFFERENT NUMBER OF BS ANTENNAS.	38
FIGURE 16: MMSE SINGLE CELL SCENARIO AND PERFECT CSI.....	46
FIGURE 17: MAXIMAL EE FOR DIFFERENT NUMBER OF BS ANTENNAS AND DIFFERENT PROCESSING SCHEMES IN THE SINGLE-CELL SCENARIO.	48
FIGURE 18: TOTAL RF POWER AT THE EE-MAXIMIZING SOLUTION FOR DIFFERENT NUMBER OF BS ANTENNAS IN THE SINGLE-CELL SCENARIO. THE RADIATED POWER PER BS ANTENNA IS ALSO SHOWN.	49
FIGURE 19: AREA THROUGHPUT AT THE EE-MAXIMIZING SOLUTION FOR DIFFERENT NUMBER OF BS ANTENNAS IN THE SINGLE-CELL SCENARIO.....	50

LIST O F TABLES

TABLE 1: SIMULATION PARAMETERS.....	28
TABLE 2: : CIRCUIT POWER COEFFICIENT FOR ZF PROCESSING.....	29
TABLE 3: : CIRCUIT POWER COEFFICIENT FOR MRT/MRC PROCESSING.....	32
TABLE 4: : CIRCUIT POWER COEFFICIENT FOR MMSE PROCESSING.....	43
TABLE 5: POWER CONSUMPTION PARAMETERS VALUES.....	44

KEY TO ABBREVIATIONS AND SYMBOLS

σ_t	delay spread
B_c	Coherence bandwidth
T_c	Coherence time
B_s	Signal bandwidth
f_m/B_d	Doppler Shift
T_s	Symbol time
$\bar{\tau}$	Excess delay
G_t/G_r	Gain of transmitter / receiver
X^H	Hermition
P_r	Receive power
P_t	Transmit power
PL	Path loss
X^T	Transpose
\hat{X}	Estimate
$\ \quad \ $	Euclidean norm
$ \quad $	Absolute value
MIMO	Multiple Input Multiple Output
SNR	Signal to noise ratio
RF	Radio frequency
EE	Energy efficiency
OPEX	Operational Expenditure
BS	Base Station
ARPU	Average Revenue per User
3G/4G	3 rd / 4 th Generation
3GPP	3 rd Generation Partnership Project
SE	Spectral Efficiency
GSM	Global System for Mobiles
LTE	Long term Evolution

AWGN	Additive White Gaussian Noise
BC	Broadcast Channel
UMTS	Universal Mobile Telecommunication System
BW	Band Width
SDR	Software Defined Radio
SCAs	Small-cell Access Points
RZF	Regularized Zero Forcing
MU-MIMO	Multi-user MIMO
LOS	Line of Sight
Tx	Transmitter
Rx	Receiver
ISI	Inter Symbol Interference
SIMO	Single Input Multiple Output
MMSE	Minimum mean Square Error
OFDM	Orthogonal Frequency Division Multiplexing
P2P	Point to Point
CCI	Co Channel Interference
CDMA	Code Division Multiple Access
CSI	Channel State Information
CSIR	CSI at Receiver
MRC	Maximal Ratio Combining
BER	Bit Error Rate
ML	Maximum Likelihood
SIC	Successive Interference Cancellation
MAC	Multiple Access Channel
UL	UP Link
DL	Down Link
MS	Mobile Station
MSC	Mobile Switching Centre
TDD	Time Division Duplex
MRT	Maximal Ratio Transmission
LO	Local Oscillator

DAC	Digital to Analog Convert
LNA	low-noise amplifier
IFA	intermediate frequency amplifier
ADC	Analog to Digital
MT	Mobile Telephones

Introduction

Energy efficiency (EE) and high data rates are the main driving forces for the evolution of wireless communication systems. More requirement in capacity in wireless networks will further increase the circuit power consumption and reduces EE. Traditionally, these requirements have been fulfilled by increasing both the transmit power and the bandwidth [1]. However, radio spectrum available for wireless services is extremely scarce and universal frequency reuse is a new trend to accommodate the increasing number of users. In other words, increasing the transmission bandwidth will not always be an option in the future [2]. On the other hand, power consumption in cellular networks is not only a financial burden to the service providers, but also one of the main sources of greenhouse gas emission [3]. Besides, due to the universal frequency reuse, strong co-channel interference puts system designers in a dilemma since increasing the transmit power may not be beneficial to the overall system performance [2]. In this circumstance, intelligent design for system optimization under different service requirements is immediately needed. As a consequence, a better system design for utilizing the limited resources is needed [3, 4]. So optimal EE and minimizing power consumption at base station (BS) using optimum algorithms are considered viable solutions to achieve afore mentioned objectives.

1.1 How Mobile Data Traffic effects Energy Efficiency?

With the expansion of population, the number of mobile users are also increasing, implying a growth in demand for communications services and increased capacity. Besides, it is noticed that the population density is geographically-dependent. Thus, to achieve higher technical and economic performance, different strategies may be applicable to different scenarios. For high-density areas, increased number of links will cause severe interference, which significantly degrades quality of service. High energy consumption also challenges the power limits of communication devices [3]. For low-density areas, inefficient use of wireless devices makes communication expensive, due to the high cost in enabling and maintaining effective long distance communications. At the same time, wireless technologies are continually evolving, adapting to the new requirements in modern communications. So the emergence of mobile communications, both the density of mobile devices and the number have constantly increased. An assumption was made that a trillion devices will be connected to the Internet by the end of 2013 [5], with a growing share of these on mobile networks. Figure 1 shows a forecast of the resulting mobile traffic until 2017. To provide facility to this growing traffic load, the rate, size and density of the infrastructure network are continually upgraded by network operators. Deploying more BS antennas to fulfill the demand for more capacity increases Operational cost (OPEX) growing energy prices. It is required to design a wireless network that minimizes the overall cost and enhance the average revenue per user (ARPU) and also fulfill the demand for capacity.

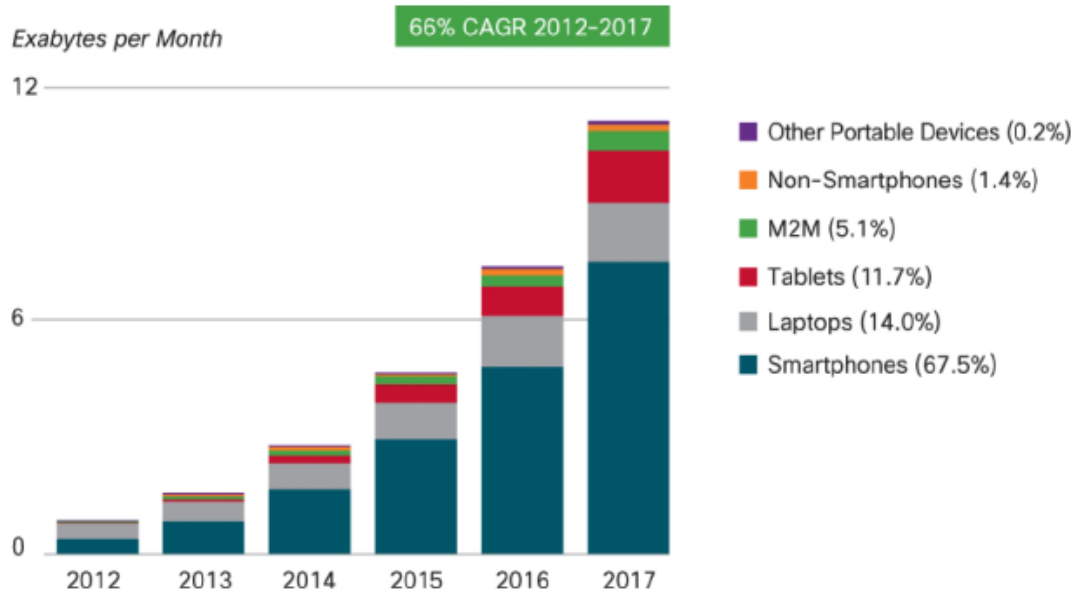


Figure 1: Mobile traffic forecast 2012-2017 with a Compound Annual Growth [5].

1.2 Why Energy Efficiency?

a. An exponential growth in traffic required more capacity in wireless access networks, implying a growth in demand for communications services and increase in capacity will increase total power consumption. By increasing more number of base station (BS) will increase the overall energy cost [6]. Previous technology based infrastructure e.g., 3G and 4G standards have less spectrum efficiency and high cost based BS but now evolution of spectrum efficiency energy and cost efficiency are also considered. Downlink SE of 3GPP increases from 0.05 b/s/Hz to 5 b/s/Hz as the system evolves from GSM to LTE [6, 7]. In future system deployment has to balance cost efficiency and energy efficiency. Improvements in electronics and digital communications

system reduces the power consumption in the base station. These improvements are not enough to fulfill the requirement of increase in energy consumption cause by demands for more capacity [8].

b. Besides EE energy preserving can also plays a critical role in mobile device because advancement in technology, battery i.e. used for energy saving has not with us with the growing demand of more capacity. EE communication is also compulsory to reduce inter-cell interference and to reduce environmental impacts (heat dissipation and electronic pollution) [6, 7].

c. The development of the circuit power consumption constantly increased by increasing in number of antennas (e.g., the radio frequency (RF) circuit power consumption, as well as the transmit power consumption should be considered as a key) [8]. Distribution of the circuit power consumption increases according to the increment of the number of transmit antennas hence, \ the total power consumption is also proportionally increasing [9].

d. Before discussion of the EE system should be spectrum and cost efficient. Later GSM and UMTS uses fixed transmission BW, leaving no space for dynamic BW adjustment. Future deployment of LTE or LTE-Advanced systems are more spectrum efficient with the growing demand for more capacity. However, technologies (e.g., Spectrum reframing, Carrier aggression and Software defined radio (SDR)-based CR techniques) are maturing to support the flexible use of BW. With implementation of energy efficient technologies extra overhead will use in practical systems. For example, CA requires multiple radio frequency chains and CR needs additional energy for sensing. So

we have to pay more attention on how to make system more energy efficient as well as spectrum and cost efficient [6].

e. Multiplexing gain Increasing using more number of transmit and receive antennas but size of overhead also increases [10, 6].

1.2.1 Solutions Available

Several studies on the subject have been done and various solutions to the problem published so far are enumerated:

- a. Today's latest technology is more energy efficient and less power consumption. Using more efficient technology make system more reliable and easy for user and reducing the power consumption of the main consumer, for example, by using more efficient devices or more advanced techniques to adapt the power consumption to the traffic situation [6, 8].
- b. By applying power saving network deployment strategies, e.g., power is saved by carefully accommodating the deployment of small low-power base stations to the traffic requirements. Various areas e.g., in hot spot areas where traffic density is high, the density of base stations will be high, whereas in rural areas only a few macro base stations are needed to provide coverage [6, 12]. To reduce infrastructure cost and manage spectrum is another technique but which density of base stations should be used to minimize power consumption in each area type is anonymous. Although the transmitter power can be reduced in small cells, this is counteracted by the increased number of base stations (cells), and it is not obvious how the total power consumption is decrease [8].
- c. Turn off part of the circuit operations when some antennas are not used to reduce the circuit power consumption, few antennas should not be used even when they have good

channel states (CSI) [11] because these antennas consumes too much circuit power. The problem is non-concave and multiple local maximums may exist but develop some algorithms that converge to global optimum [11].

- d. Deployment of small cells to reduce some burden from BS employ that most data traffic is localized and requested by low mobility users. This approach reduces the average distance between transmitter and receiver, which translate into lower propagation losses and higher energy efficiency (EE) [12].
- e. By combining small cell and massive mimo power consumption can be reduced [12]. Networks provide great improvements in dynamic power consumption but required more hardware and therefore increase the static power consumption. In other words, dense network topologies must be properly deployed and optimized to actually improve the overall energy efficiency [8]. Major benefits are also achievable by low complexity beam forming algorithms e.g., the RZF beam forming algorithm [12].

1.2.2 Reason/ Justification for the Selection of the Topic

Ever growing demand for more capacity in wireless networks will further increase the energy consumption as well as increases the energy cost. It is required to maintain capacity and to limit the cost. 3G and 4G standards have not dynamic range in spectrum. They have spectrum shortage and high cost base station sites, but these systems are designed for extreme spectrum efficiency [6, 7]. 3G has a spectral efficiency approximately 10 times that of a 2G system [8]. Massive MIMO can be rightly considered to be beyond 4G due to its advantages. The better utilization of the system can only be achieved through energy efficient communication. This research work will provide the optimum solution

related to deployment of energy efficient Massive MIMO system at limited cost. This area is still new and needs to be further explored for an optimum solution.

1.2.3 Proposed Solution

This thesis will investigate various methods available for achieving EE. The EE is defined as the ratio of achievable capacity to the total average power consumption. It is measured in bit/Joule [8].

$$EE = \frac{\text{Average Sum Throughput} \left[\frac{\text{bit}}{\text{channel use}} \right]}{\text{Power Consumption} \left[\frac{\text{Joule}}{\text{channel use}} \right]}$$

Conventional approach is to maximize throughput with fixed power or minimize transmit power for fixed throughput however, for effective EE there is a requirement of creating a balance in throughput and power consumption which can provide an optimal EE solution. This thesis will evaluate a detailed power consumption model and will incorporate overheads due to signaling while calculating EE for massive MIMO systems.

1.3 Methodology

This section describes the general research approach and how the scope of the work was bounded. In a mobile communications network, it is estimated that base stations contribute between 60-80% of the overall energy consumption [8-9]. The base station energy dissipation constitutes both load dependent (Radio Head and Radio Frequency energy) and load independent (Overhead energy) components. This research focused on the energy consumption with particular emphasis on Radio Frequency (RF) downlink transmissions. We consider (DL) downlink at the BS and use different precoding schemes at the BS. We propose a new detailed power consumption model that shows how active

users, optimal number of antennas, and transmit power affect the EE. During this research phase, the performance evaluation of the EE was developed in MATLAB.

1.4 Organization

Chapter 2 presents some MIMO, MU MIMO and Massive MIMO. In chapter 3 power consumption is proposed. In chapter 4 optimum energy efficiency is discussed with different processing schemes. In chapter 5 the simulation results will be presented and in last chapter conclusion and few words about future goals are covered.

1.5 Notation

Following notations are used in in this thesis:

- a. Italic letters are used for symbols.
- b. Small italic bold letters are used for vectors.
- c. Capital bold are used as matrices.
- d. Vector and matrices having entries that belong to the set of real numbers is represented by $\in \mathbb{R}$.

MIMO, Multi User MIMO and Massive MIMO

2.1 MIMO - An overview

A wireless network uses multiple Tx and Rx antennas is basically called a MIMO system (multiple input and multiple output). MIMO technology increases both network capacity and range of wireless network. MIMO channel can use different paths for propagation. This improve the diversity gain and multiplexing gain [14, 15]. The main design goals behind the fourth generation (4G) of wireless systems are higher user bit rates, lower delays and increased energy efficiency. These requirements call for new techniques to enhance the communications systems performance. The use of multiple antennas at both the transmitter and receiver side has result in a useful technique to improve the performance of wireless systems in terms of capacity and reliability [16]. In this section the concept of multiple input multiple Output (MIMO) system will be introduced. Furthermore, we will study the concepts of spatial multiplexing and spatial diversity in MIMO communication systems.

We focus on the MIMO system presented in Figure 2 where the multiple transmitter is equipped with M_T transmit antennas and the receiver with N_R antennas. A Rayleigh fading channel is considered, figure for MIMO system can be represented as:

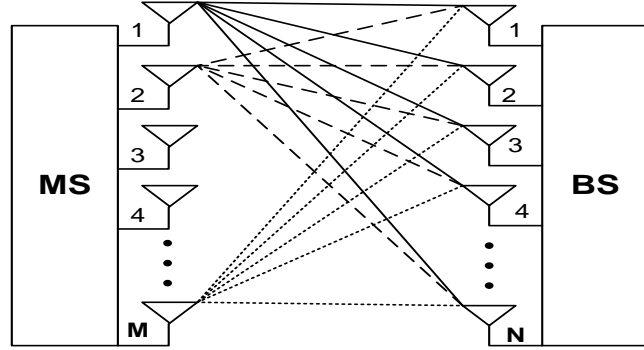


Figure 2: MIMO System for multiple Transmit and Receive Antennas

Wireless channel matrix \mathbf{H} for $[N \times M]$ MIMO system is given below. The subscript i and j for h_{ij} mean the channel for the i th receive antenna to the j th transmit antenna in a MIMO system.

$$\mathbf{H} = \begin{bmatrix} h_{11} & h_{12} & \dots & h_{1M} \\ h_{21} & h_{22} & \dots & h_{2M} \\ \vdots & \vdots & \ddots & \vdots \\ h_{N1} & h_{N2} & \dots & h_{NM} \end{bmatrix}_{N \times M} \quad (2.1)$$

where each matrix element defines a Zero Mean Circular Symmetric Complex Gaussian random variable with unit variance. The input output relation of the system shown in Figure 2 is given by:

$$\bar{\mathbf{Y}} = \mathbf{H}\bar{\mathbf{X}} + \bar{\mathbf{n}} \quad (2.2)$$

where $\bar{\mathbf{Y}}$ is received signal vector, $\bar{\mathbf{X}}$ is transmitted signal vector, \mathbf{H} is channel matrix and $\bar{\mathbf{n}}$ is Additive White Gaussian noise (AWGN).

2.2 Spatial Multiplexing Gain

A spatial multiplexing system divides a higher data rate stream into multiple low data rate streams and modulates them into independent signals which are transmitted simultaneously within the same frequency band using multiple antennas. This technique

allows a boost of supportable data rate of the channel linearly proportional to the number of antennas thus it provides improvement in spectral efficiency of the system with increased bandwidth utilization. The number of supportable independent signals is always less than or equal to the number of antennas, for systems with asymmetric number of antennas at both ends the number of signals is limited by the lesser number of antennas [17].

The spatial multiplexing system can properly function only if the signals from different antennas are uncorrelated. Fortunately multipath fading, which has traditionally acted as hindrance for communication systems provides necessary de-correlation for the signal as they propagate towards the receiver. In terms of MIMO equation model, this corresponds to a non-singular channel matrix which allows the linear equation system for MIMO to be solved. If there exists correlation among the signals, the channel matrix would have dependent rows or columns and will be non-invertible [17].

2.2.1 Spatial Multiplexing Receivers

The optimal decoding of the received signals with Maximum Likelihood (ML) like in SISO systems is prohibitively complex even for small number of antennas. If the alphabet size of the used constellation is given by M , the ML decoding involves exhaustive search over a vector space of size M^{N_T} . This is because unlike SISO systems, MIMO transmitters transmit symbol vectors instead of simple scalar symbols. There are multiple detection algorithms for MIMO available such as Zero Forcing (ZF), Minimum Mean Squared error (MMSE), ML, Sphere Decoding etc. The primary MIMO spatial multiplexing specific detectors that can be taken as representatives of their classification

are Successive Interference Cancellation (SIC) and Sphere Decoding algorithm, both are elaborated here [17].

2.2.2 Successive Interference Cancellation

Linear detection algorithms such as ZF and MMSE provide poor performance but with an advantage of less computational complexity, non-linear detection algorithms have the opposite traits. A balance between the two in terms of complexity and performance is achieved by SIC algorithm. It is an iterative procedure that involves a bank of multiple linear detectors. The signals from different transmitter antennas are individually detected with successive cancellation of the detected signal effect from the received signal. The successive cancellation is done by subtracting the detected symbol from the received signal at each step after multiplication with the corresponding channel matrix column. This results in a modified received vector with reduced interference at the subsequent stages [13]. An important aspect of SIC architecture is exploitation of timing synchronization of the received signal, since this is characteristic of BLAST transmitters and the spatial difference between transmitter antennas. The order in which the signals are detected and cancelled has major effect on system performance. Some ordering techniques are Signal to Noise Ratio (SNR) based ordering, Signal to Interference Noise Ratio (SINR) based ordering, channel norm based ordering and simple signal reception based ordering [13].

2.3 Spatial Diversity

The spatial diversity architecture of MIMO provides gain in terms of link robustness, coverage area and transmit power needed for a particular SNR level. The basic conception behind spatial diversity is the independent fading of the multiple signal paths

between different transmitter and receiver antenna pairs. It is extremely less probable for all the signal paths to face deep fade simultaneously. Thus the diversity system uses all the $N_R \times N_T$ signal paths for diversity benefits. This section elaborates the transmit and receive diversity aspects separately along with the corresponding algorithms [17].

2.3.1 Transmit Diversity

Transmit diversity techniques use multiple antennas at the transmitter to achieve diversity gain. Diversity is introduced here by transmitting redundantly transmit same signal from multiple transmitting antennas. It is quite less likely for all the transmitted signals to face deep fading at the same time so this aspects provides for the diversity in this architecture. Mainly two different types of algorithms can be used for transmit diversity depending upon state of channel knowledge at the transmitter. For CSIT available, transmit beamforming is used. For non-availability of CSIT, space time coding is used specifically Alamouti coding is elaborated here along with necessary mathematical explanation [13, 19].

2.3.2 Receive Diversity

Receive diversity combines the independently faded signal paths associated with signals by different receiving antennas to achieve a better resultant signal which is then decoded using conventional algorithms. It is based on the concept of combining the signals from different receiver antennas in hope that some of the signals are always in better conditions in terms of fading. An important aspect of receive diversity is the process of co-phasing the multiple signals which need to be combined, because only then will they add up constructively and provide diversity gain. Some of the important receive diversity

algorithms explained here are: selection combining, threshold combining, maximal ratio combining and equal gain combining [18].

a. Selection Combining (SC). The selection combining algorithm selects the signal from the antenna which has received the highest SNR signal. Thus with selection combining the output SNR is equal to the maximum of the SNRs of all the receiving antennas. Since only one signal is selected, the selection combining algorithm needs only one receiver to demodulate the final signal. Furthermore, since only one antenna signal is used, there is no need for co-phasing procedure. For further details see [13].

b. Threshold Combining (TC). An important drawback of the selection combining is the need for multiple receivers to continuously monitor SNR for all antennas for the case where the system involves continuous transmissions. This requirement is bypassed by the threshold combining algorithm where the receiver sequentially scans all the receiving antennas and selects the first signal it finds with SNR greater than a specified threshold. The service duration of the selected antenna remains valid till its SNR remains higher than the SNR threshold, after that the receiver switches to another branch which might be selected randomly. Like selection combining, signal for only one antenna is selected so co-phasing is not needed [13].

c. Maximal Ratio Combining (MRC) The basic concept of maximal ratio combining is to combine all the received signals, usually through averaging, in order to generate an estimate of the transmitted signal. In all the receiver combining techniques mentioned before, the output signal comprises of signal from only one of the antennas, but in maximal ratio combining, the final signal comprises of a linear combination of all the input signals. Since multiple signals are combined here, maximal ratio combining needs

co-phasing of the signals before combining them. Thus the output signal is sum of products of individual signals with their corresponding weights [13]. The weights need to be selected in order to maximize the overall SNR of the output signal. This implies that the weights of the individual signals should be proportional to their SNR. The superior performance of maximal ratio combining is shown by the fact that its average SNR increases linearly with the number of receiver antennas. This is because the final output SNR is equal to the sum of individual signal SNR [13].

d. Equal Gain Combining (EGC)

The superior performance of maximal ratio combining comes with a complexity of determining time varying SNR of each individual signals. A simpler technique is to combine all the signals with equal weights irrespective of their SNR. Equal gain combining also needs the signals to be added with co-phasing like in maximal ratio combining. The performance is slightly degrades but there is no need for SNR determination in equal gain combining. Thus equal gain combining technique provides a less complex alternative as compares to maximal ratio combining with somewhat less performance.

2.4 Massive MIMO

Massive MIMO paradigm is an evolution of multi-user MIMO (MU-MIMO). It should be understood that MIMO, in current wireless standards such as LTE is typically implemented in its single-user form. That is to say that on a given channel and in a given timeslot, all the base station antennas are used to communicate with a single user terminal, itself being equipped with multiple antennas, where the multiplicity of antennas at both ends allows the creation of multiple data streams in space, thus multiplying the link

capacity by a significant factor. As it is easier to have a lot of antennas (for size and cost reasons) at the base station compared to the handset, these additional degrees of freedom can be used to communicate with multiple users at the same time, giving rise to MU-MIMO [20]. However, this is a much more difficult problem given that the multiple users addressed simultaneously cannot easily perform joint processing in order to eliminate the inter-user interference created with this method. Therefore, while MU-MIMO is supported in LTE release 8, the precoding scheme therein does not completely address the interference problem. It follows that efficient implementation requires clever processing beyond what is dictated by the standard, and many system designers are skeptical with this route. The reason is that it is much simpler to maximize single-user MIMO (SU-MIMO) throughput, thus liberating the channels sooner for other users, rather than attempt MU-MIMO while the system gains are similar. Given this state of affairs, neither SU-MIMO nor MU-MIMO is sufficiently powerful to achieve the 1000's of capacity increase demanded by 5G. [21] introduced the concept of "massive MIMO" in 2010 (also referred to as large-scale antenna systems or LSAS), generating immediate interest and numerous other papers [22, 23]. It constitutes a theoretical and asymptotic analysis of a multi-cell scenario where a population of single-antenna terminals are served by cellular base stations having an infinite number of antennas. While some real-world constraints are not considered, this work provides useful insights into the benefits and drawbacks of LSAS. Namely, when the number of base station antennas is allowed to tend towards infinity,

1. The effect of uncorrelated noise and fast fading vanish;
2. Throughput and the number of terminals become independent from the size of the cells;

3. The required transmitted energy tends towards zero (due to infinite array gain);
4. Multi-user interference vanishes; and
5. Very simple forms of detection and precoding, namely matched filtering and Eigen beamforming, become optimal.

However, such theoretical fundamental benefits cannot be achieved without overcoming multiple practical hurdles. Known issues affecting massive MIMO include,

- a. Pilot contamination:** In massive MIMO, it is unrealistic to operate in FDD mode and to use some sort of sounding / feedback technique to obtain downlink channel estimates, given the staggering overhead this would entail for such a large array. TDD operation is generally assumed, with a frame size such that decent downlink channel estimates can be obtained by reciprocity from the uplink channel estimates. Typically, the latter are obtained during a dedicated training interval, or, equivalently using pilot symbols. The pilots or training sequences can be made orthogonal or quasi-orthogonal among users for a single cell, but will necessarily be contaminated by transmissions (re-use of training sequences) from surrounding cells. This effect, which does not diminish with the size of the array L , is widely recognized as one of the main practical capacity limitations of the massive MIMO paradigm.
- b. Array scale:** The sheer array scale required to achieve the true massive effect, whereby Eigen beamforming and maximal-ratio combining can be leveraged, involves staggering size, cost, and energy consumption considerations.

- c. **Array coherence:** Appropriate synchronization, calibration, and phase alignment across a large-scale array, of hundreds of antennas or more, pose serious practical challenges. Figure3 below shows a simple Massive MIMO system.

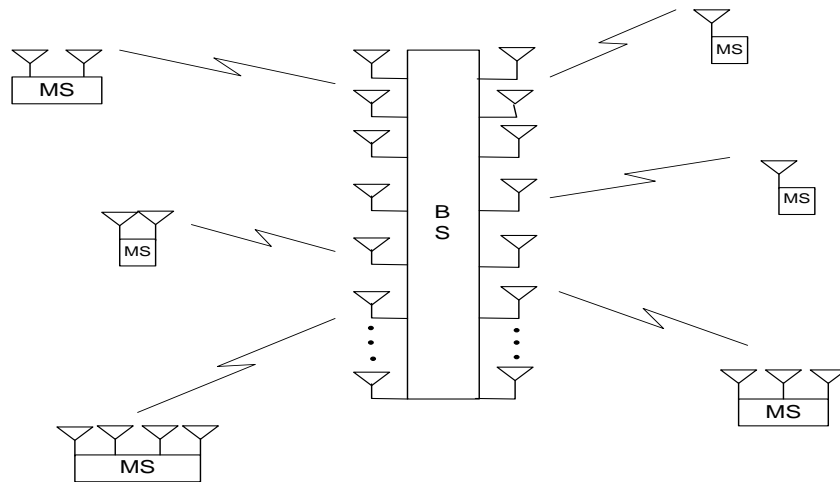


Figure 3: A simplified Massive MIMO System

2.5 Summary

The MIMO wireless system is elaborated extensively in this chapter. The architecture of MIMO system is elaborated with mathematical background. The aspect of spatial multiplexing and spatial diversity are separately explained. Emphasis is mostly put on the generally used algorithms pertaining to spatial multiplexing and spatial diversity techniques. The algorithms are elaborated with classification between those used at the transmitter side and those used at the receiver side. At the end Massive MIMO basic concept is discussed.

Energy Efficiency

3.1 Introduction to Energy Efficiency

Power consumption has a direct impact on energy consumption. Power reductions, as well as energy efficiency are critical factors. The MT's active mode power consumption is not the only property critical from energy efficiency standpoint – throughput (*e.g. Joules/Mbit*) also plays an important role. Regrettably, the energy efficiency of BSs is exceptionally poor in these circumstances. We start with analyzing cellular network energy consumption. Based on the results shown in Figure 4, radio base stations are identified to be the most energy-consuming components, which use about 57% of the total network power. The energy spent on mobile switching, core transmission, data center and retail is about 20%, 15%, 6% and 2% respectively [24-26]. Therefore, currently most energy-efficient designs are targeted towards radio base stations.

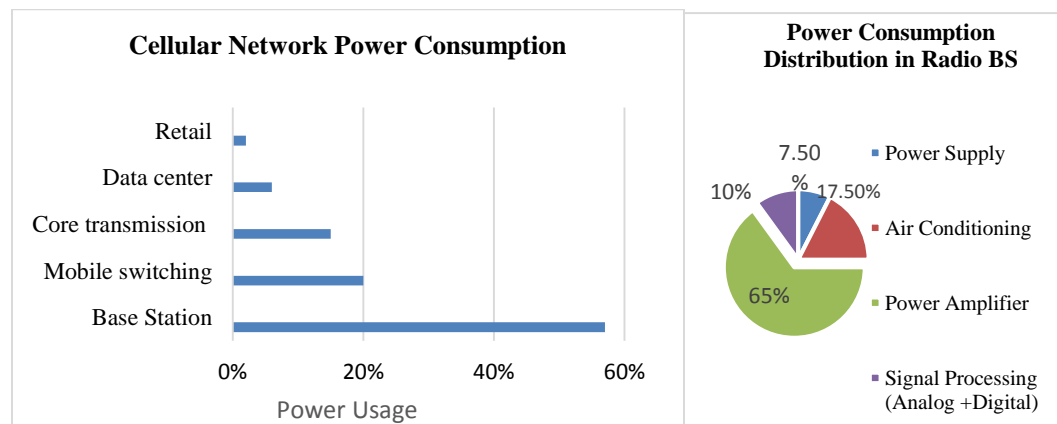


Figure 4: Cellular Network Power Consumption and Circuit Power Consumption at Base Stations [26]

Inefficiencies can be further classify as [26, 27]

a. Component level

Efficiency of the analog components e.g., power amplifier (PA) reduces power at its output.

b. Link level

Information signals, synchronization, and pilot overheads are transmitted continuously. This demand that BS are incessantly on.

c. Network level

Wireless network deployment paradigm with large macrocells in it needs small cells to supplement and fulfil the peak capacity demand. This is however rather static topology and doesn't therefore adapt very well to low load situations.

Figure below illustrates the monotonicity of energy efficiency in a single carrier system. Taking the total power consumption into consideration, energy efficiency can be define as the ratio of the average rate throughput and power consumption. Interestingly, introduction of total power consumption transforms the energy efficiency-versus-SNR curve from a monotonic decreasing function to a function with a bell shape curve.

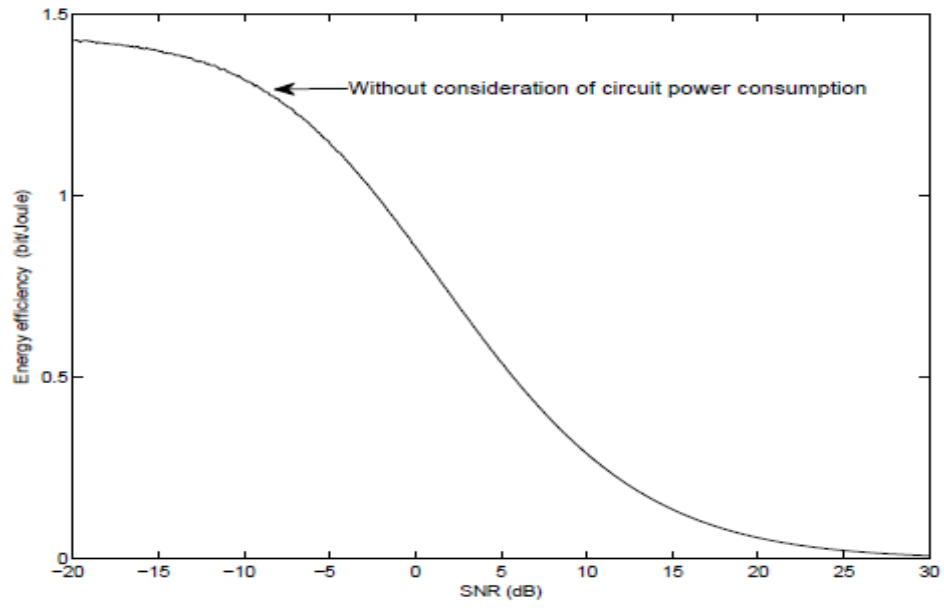


Figure 5: EE versus SNR without consideration of circuit power consumption.

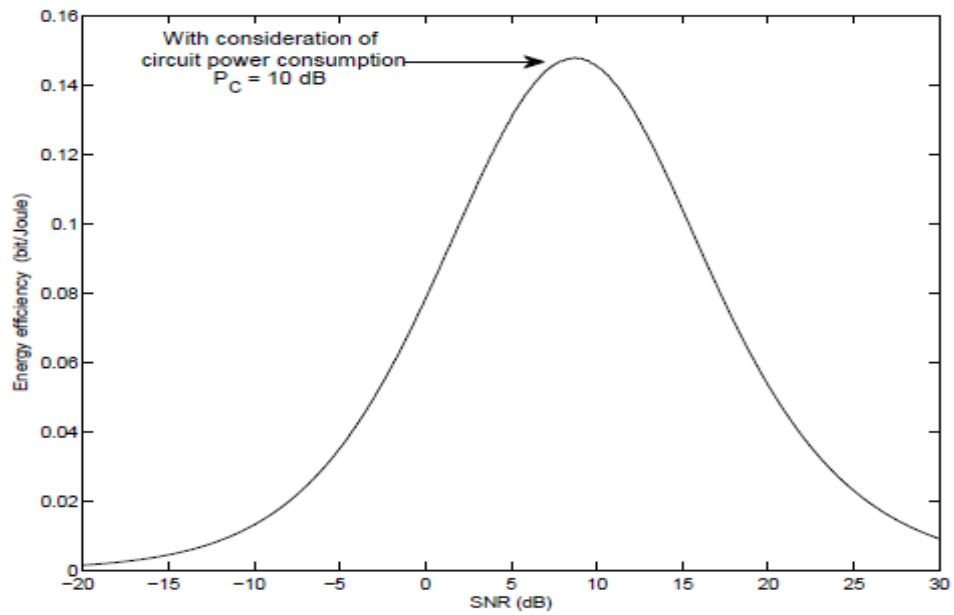


Figure 6: EE versus SNR with consideration of circuit power consumption.

Figures above shown an illustration of energy efficiency (EE) versus SNR using Rayleigh fading and power consumption ($P_C = 10$ dB) with circuit power consumption consideration.

Respect to SNR, Figure 6. In other words, transmission with an arbitrarily low power, i.e., $P \rightarrow 0$, may no longer be the best option for maximizing the energy efficiency for the case of $P_C > 0$. As a result, increasing transmit antennas also increase in the maximum energy efficiency which should be taken into account for resource allocation algorithm design.

3.2 Circuit power consumption model

For design of generic total power consumption modeling it is assumed that (circuit power consumption) P_{CP} is the sum of the power consumed by different analog components and digital signal processing [28]. Circuit power consumption model for the MU-MIMO system under investigation [10];

$$P_{CP} = P_{FIX} + P_{TC} + P_{CE} + P_{C/D} + P_{BH} + P_{LP}, \quad (3.1)$$

where P_{FIX} is fix power i.e. consumed power in analog devices (e.g., baseband processors, load-independent power of backhaul infrastructure, site-cooling and control signaling). P_{TC} is the power consumption of the Tx and Rx. P_{CE} is the power used in channel estimation, $P_{C/D}$ is power required for the channel coding and decoding, P_{BH} is load dependent backhaul and P_{LP} is the power required for computation of MMSE processing. Detail of this model is discussed in chapter 5.

3.3 Summary

Chapter elaborates EE and architecture of BS power consumption system model. Initially, analyzing cellular network energy consumption as EE has direct link with power consumption then introduction to the power consumption transforms the energy efficiency-versus-SNR curve was discussed. In the next chapter simulation and results will be discuss.

Optimum EE in Massive MIMO using MRT and ZF Precoding

4.1 Problem Formulation

The network is consider as follows. BS having M antennas communicate with K user. We consider a single cell network for both UL and DL with operating bandwidth of B Hz. All users i.e. $K = \{1 \dots k\}$ are selected in round robin fashion. The channel is subject to block fading with coherence bandwidth (B_c in Hz) and coherence time (T_c). Time slots are selected in such a way that users and BS are perfectly synchronized and operate according to the TDD protocol shown in Figure 7. Users channel are assumed to be static within the frequency $U = B_c T_c$.

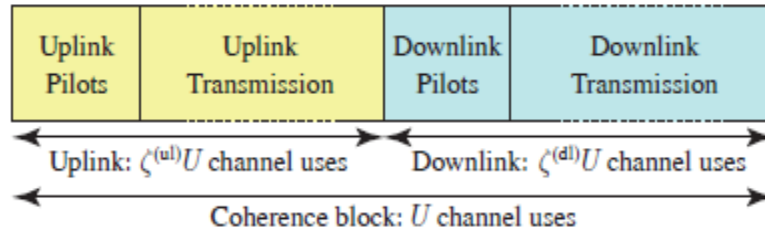


Figure 7: Illustration of the TDD protocol

Figure 7 shows the UL and DL transmission using TDD protocol. We consider jointly UL and DL and fixed ratios of DL and UL transmission are denoted by $\zeta^{(ul)}$ and $\zeta^{(dl)}$ respectively, with $\zeta^{(ul)} + \zeta^{(dl)} = 1$. From figure 7, UL transmission takes place first and consists of $U\zeta^{(ul)}$ channel uses and after that DL transmission take place . Pilot signaling

occupies $\tau^{(ul)}$ K channel uses in the UL and $\tau^{(dl)}$ K in the DL

Figure 8 shows the user density of the coverage area. Physical location of user k is denoted by $x_k \in \mathbb{R}^2$ (in meters). Function $l(\cdot): \mathbb{R}^2 \rightarrow \mathbb{R}$ shows the large-scale fading at different user locations, $l(x_k)$ is the average channel attenuation due to path-loss and shadowing at locations x_k . User are distributed using uniform distribution and selected in a round-robin fashion [10] as shown in figure.

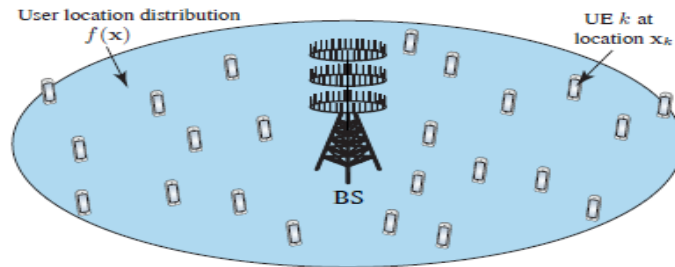


Figure 8: A generic MU- MIMO scenario.

4.2 EE Metrics

In order to meet the performance of energy efficient solutions, it is important to identify suitable metrics to understand what gains are achieved. Since, the concept of energy efficiency only becomes meaningful when is measured, energy efficient metrics should provide quantified information to evaluate efficiency. Energy efficiency metrics are mainly used for three proposes:

- to compare the difference in power consumption between components and systems of the same class;
- to set specific long term targets in research and development;

- to allow the optimization of current communication systems based on energy efficiency constrains.

Energy efficiency metrics have been widely discussed in literature, thus for this work there are two particular important metrics that we will use. The first and absolute metric can be define as the average information rate and the total circuit power consumption [8].

$$EE = \frac{\text{Average Sum Throughput} \left[\frac{\text{bit}}{\text{channel use}} \right]}{\text{Power Consumption} \left[\frac{\text{Joule}}{\text{channel use}} \right]}$$

In a MU-MIMO total EE for UL and DL takes the following form [10];

$$EE = \frac{\sum_{k=1}^K \{ (R_k^{ul}) + (R_k^{dl}) \}}{P_{TX}^{ul} + P_{TX}^{dl} + P_{CP}}, \quad (4.1)$$

where R_k^{ul} and R_k^{dl} are UL and DL rates of each user. P_{TX}^{ul}, P_{TX}^{dl} are uplink and downlink powers and P_{CP} accounts for the circuit power consumption.

For the design of EE communication system it is required to model circuit power consumption P_{CP} . Our aims is to provide an appropriate model for P_{CP} with linear precoding.

4.2.1 Linear Processing

Tx and Rx vectors of information symbols at the BS are generated by transmit precoding and processed by receive combining, respectively. P_{LPC} used in equation (4.5) is the power

required for the computation of \mathbf{G} and \mathbf{V} . Where \mathbf{G} and \mathbf{V} are the precoding and combining matrices and the complexity depends on MRT and ZF processing scheme respectively [13];

$$\mathbf{G} = \begin{cases} \mathbf{H}_{[K \times M]} \text{ for MRT,} \\ \mathbf{H}_{[K \times M]} (\mathbf{H}_{[K \times M]} \mathbf{H}_{[M \times K]}^H)^{-1} \text{ for ZF,} \end{cases} \quad (4.2)$$

and

$$\mathbf{V} = \begin{cases} \mathbf{H}_{[K \times M]} \text{ for MRT,} \\ \mathbf{H}_{[K \times M]} (\mathbf{H}_{[K \times M]} \mathbf{H}_{[M \times K]}^H)^{-1} \text{ for ZF,} \end{cases} \quad (4.3)$$

As we considered UL and DL are same so by using $\mathbf{G} = \mathbf{V}$ to make our calculation more simple and easy.

For MRT/MRC there is only need to normalize each column of \mathbf{H} and approximately [33];

$$P_{LP-C}^{(MRT/MRC)} = \frac{B}{U} \frac{3MK}{L_{BS}} \quad (4.4)$$

is consumed.

Above equation is calculated using linear algebra operations in [34]. For Zero forcing processing Cholesky factorization and back-substitution is used and almost;

$$P_{LP-C}^{(ZF)} = \frac{B}{U} \left(\frac{K^3}{3L_{BS}} + \frac{3MK^2 + MK}{L_{BS}} \right) \quad (4.5)$$

is consumed.

For simulation scenario, simulation parameters are given in Table 1 using 3GPP propagation environment defined in [33], RF and baseband power modeling from [28], [31], [32], [35], P_{BH} (backhaul power) according to [36], and the computational efficiencies are from [7], [37].

Cell radius (single-cell)	250 m
Minimum distance	35 m
PA efficiency at BS	0.39
PA efficiency at UEs	0.3
Transmission bandwidth	20 MHz
Channel coherence bandwidth	180 kHz
Channel coherence time	10 ms
Coherence block (channel uses)	1800
Total noise power	-96dBm
Relative pilot length	1
Fraction of uplink transmission	0.4
Fraction of downlink transmission	0.6

Table 1: Simulation Parameters

4.3 EE Optimization with ZF processing

EE optimization is solved using ZF processing in the UL and DL for analytic convenience and also for the numerical results shown below indicates that it is close-to-optimal. Using [10];

$$P_{TX}^{ZF} = P_{TX}^{ul-ZF} + P_{TX}^{dl-ZF} = \frac{B\sigma^2\alpha S_x}{\eta} K, \quad (4.6)$$

with

$$\eta = \left(\frac{\zeta^{ul}}{\eta^{ul}} + \frac{\zeta^{dl}}{\eta^{dl}} \right)^{-1}. \quad (4.7)$$

It follows that, for ZF processing, reduces to

$$EE^{ZF} = \frac{K(1 - \frac{(\tau^{(ul)} + \tau^{(dl)})K}{U})\bar{R}}{\frac{B\sigma^2\alpha S_x}{\eta}K + P_{CP}^{ZF}}, \quad (4.8)$$

where we used $R^{ul} + R^{dl} = (1 - \frac{(\tau^{(ul)} + \tau^{(dl)})K}{U})\bar{R}$ and since $\zeta^{ul} + \zeta^{dl} = 1$

Now we define the circuit power Consumption with ZF [36];

$$P_{CP}^{ZF} = P_{FIX} + P_{TC} + P_{CE} + P_{C/D} + P_{BH} + P_{LP}^{ZF}. \quad (4.9)$$

Circuit power co-efficient calculation are discussed in detail in next chapter

$C_0 = P_{FIX} + P_{SYN}$	$A = P_{COD} + P_{DEC} + P_{BT}$
$C_1 = P_{UE}$	$D_0 = P_{BS}$
$C_2 = \frac{4B\tau^{(dl)}}{UL_{UE}}$	$D_1 = \frac{B}{L_{BS}}(2 + \frac{1}{U})$
$C_3 = \frac{B}{3UL_{BS}}$	$D_2 = \frac{B}{UL_{BS}}(3 - 2\tau^{dl})$

Table 2 : : Circuit Power Coefficient For ZF Processing

By introducing the constant coefficients A, $\{C_i\}$, and $\{D_i\}$ as reported in Table then ;

$$P_{CP}^{ZF} = \sum_{i=0}^3 C_i K_i + M \sum_{i=0}^2 D_i K_i + AK(1 - \frac{(\tau^{(ul)} + \tau^{(dl)})K}{U})\bar{R} \quad (4.10)$$

$$EE^{ZF} = \frac{K(1 - \frac{(\tau^{(ul)} + \tau^{(dl)})K}{U})\bar{R}}{\frac{B\sigma^2\alpha S_x}{\eta}K + \sum_{i=0}^3 C_i K_i + M \sum_{i=0}^2 D_i K_i + AK(1 - \frac{(\tau^{(ul)} + \tau^{(dl)})K}{U})\bar{R}} \quad (4.11)$$

where $\bar{R} = B \log(1 + \alpha(M - K))$ and is also the function of (α, M, K) .

4.4 Simulation with ZF processing

4.4.1 ZF with Perfect CSI

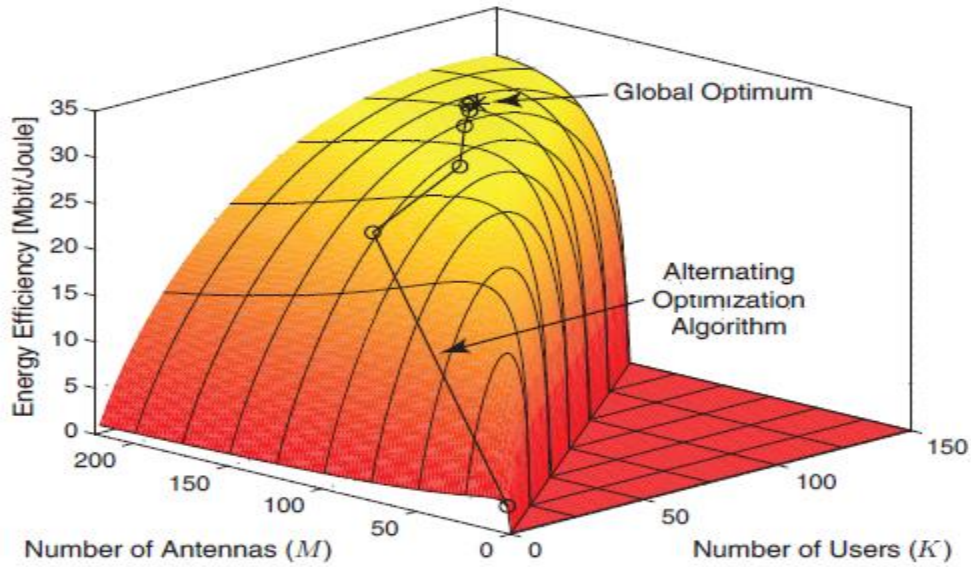


Figure 9: ZF processing single cell scenario and perfect CSI

Above figure 9 illustrated the achievable EE values for hundreds of users and BS with perfect CSI and ZF processing. Global optimum at $M = 165$ and $K = 104$, and the maximum spectral efficiency 5.7644 bit/channel use is clearly marked with star as shown

in figure. It is clearly a Massive MIMO setup and quiet smooth concave shape shows that circuit power consumption has major effect on EE curve.

4.4.2 ZF with Imperfect CSI

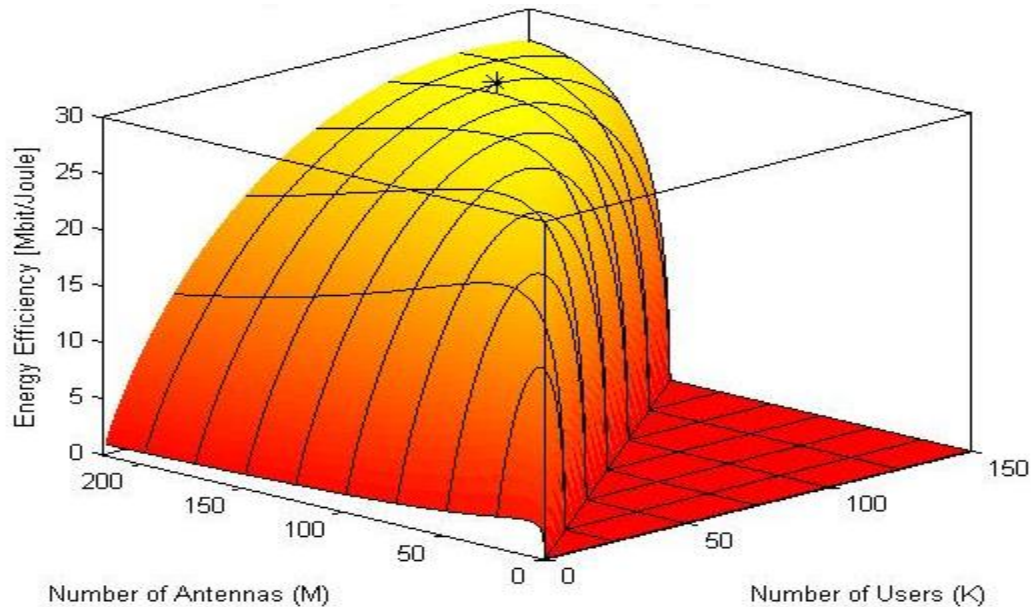


Figure 10: ZF single cell scenario and imperfect CSI

Figure 10 illustrated ZF processing under imperfect CSI with set of EE values. This figure has same behavior as above figure 9. This figure also has concave shape because of circuit power consumption and also has a global optimum and it is cleared that ZF with perfect CSI has a similar behavior as ZF with imperfect CSI.

4.5 EE Optimization with MRT/MRC processing

Now EE optimization is solved using MRT/MRC processing in the uplink and downlink. Using [10];

$$P_{TX}^{MRT/MRC} = P_{TX}^{ul-MRT/MRC} + P_{TX}^{dl-MRT/MRC} = \frac{B\sigma^2\alpha S_X}{\eta} K. \quad (4.12)$$

It follows that, for MRT/MRC processing, reduces to

$$EE^{MRT/MRC} = \frac{K(1 - \frac{(\tau^{(ul)} + \tau^{(dl)}K)}{U})\bar{R}}{\frac{B\sigma^2\alpha S_X}{\eta} K + P_{CP}^{MRT/MRC}}. \quad (4.13)$$

Now we define the circuit power Consumption with MRT/MRC

$$P_{CP}^{MRT/MRC} = P_{FIX} + P_{TC} + P_{CE} + P_{C/D} + P_{BH} + P_{LP}^{MRT/MRC}. \quad (4.14)$$

Detail Circuit power co-efficient are discussed in next chapter

$C_0 = P_{FIX} + P_{SYN}$	$A = P_{COD} + P_{DEC} + P_{BT}$
$C_1 = P_{UE}$	$D_0 = P_{BS}$
$C_2 = \frac{4B\tau^{(dl)}}{UL_{UE}}$	$D_1 = \frac{B}{L_{BS}}(2 + \frac{3}{U})$
$C_3 = 0$	$D_2 = \frac{B}{UL_{BS}}(-2\tau^{(dl)})$

Table 3: : Circuit Power Coefficient For MRT/MRC Processing

For notational convenience, we introduce the constant coefficients A, $\{C_i\}$, and $\{D_i\}$ as reported in Table then

$$P_{CP}^{MRT/MRC} = \sum_{i=0}^3 C_i K_i + M \sum_{i=0}^2 D_i K_i + AK(1 - \frac{(\tau^{(ul)} + \tau^{(dl)}K)}{U})\bar{R}, \quad (4.15)$$

where $\bar{R} = B \log(1 + \alpha(M - K))$ and is also the function of (α, M, K) and yields

$$EE^{MRT/MRC} = \frac{K(1 - \frac{(\tau^{(ul)} + \tau^{(dl)})K}{U})\bar{R}}{\frac{B\sigma^2\alpha S_x}{\eta}K + \sum_{i=0}^3 C_i K_i + M \sum_{i=0}^2 D_i K_i + AK(1 - \frac{(\tau^{(ul)} + \tau^{(dl)})K}{U})\bar{R}} \quad (4.16)$$

4.6 Simulation with MRT/MRC processing

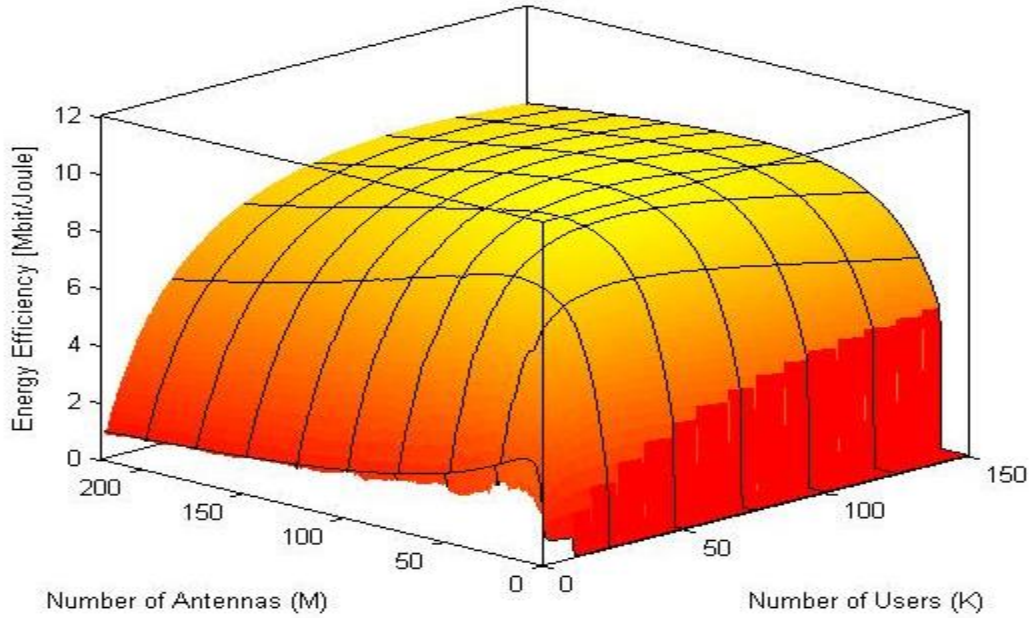


Figure 11: MRT/MRC processing with single cell scenario and perfect CSI

Interestingly, MRT/MRC processing gives a very different behavior: the EE optimum is much smaller than with ZF/MMSE and is achieved at $M = 81$ and $K = 77.6$. This can still be called a massive MIMO setup since there is a massive number of BS antennas, but it is a degenerative case where M and K are almost equal and thus the typical asymptotic massive MIMO properties from [41], [6] will not hold. The reason that $M \times K$ is that MRT/MRC operates under strong inter-user interference, thus the rate per UE is

small and it makes sense to schedule as many UEs as possible (to crank up the sum rate). The inter-user interference reduces with the number of BS antennas but we see that this asymptotic effect is not dominating over the increased computational/circuit power cost of increasing M .

4.7 Optimal Number of Users

EE-optimal value of K when M and α are given. For analytic tractability, we assume that the sum SINR αK and the number of antennas per UE M/K are kept constant and equal to $\alpha K = \bar{\alpha}$ and $\frac{M}{K} = \bar{\beta}$ with $\bar{\alpha} > 0$ and $\bar{\beta} > 1$. The gross rate is thus fixed \bar{R} at $\bar{c} = B \log(1 + \bar{\alpha}(\bar{\beta} - 1))$ and then

$$\max_{K \in \mathbb{Z}_+} \text{imize } \phi(k) = \frac{K(1 - \frac{(\tau^{(ul)} + \tau^{(dl)})K}{U})^{\bar{c}}}{\frac{B\sigma^2\alpha S_x}{\eta} \alpha + \sum_{i=0}^3 C_i K_i + \beta \sum_{i=0}^2 D_i K_{i+1} + AK(1 - \frac{(\tau^{(ul)} + \tau^{(dl)})K}{U})^{\bar{c}}}. \quad (4.17)$$

The function $\phi(k)$ is quasi-concave for $K \in \mathbb{R}$ quasi-concavity implies that the global maximizer of $\phi(k)$ for $K \in \mathbb{R}$ satisfies the stationarity condition $\frac{\partial}{\partial K} \phi(k) = 0$, which is equivalent to finding the roots of the quartic polynomial [38]. This equation shows that the optimal K is a root to the quartic polynomial A basic property in linear algebra is that quartic polynomials have exactly 4 roots (some can be complex-valued) and there are generic closed-form root expressions [39]. Unfortunately, these expressions are very lengthy. Closed form expressions are seldom used because there are simple algorithms to find the roots with higher numerical accuracy [40].

4.8 Optimal Number of BS Antennas

We now look for the $M \times K + 1$ that maximizes the EE for convenience, divide by K

$$C' = \frac{\sum_{i=0}^3 C_i K^i}{K} \quad \text{and} \quad D' = \frac{\sum_{i=0}^2 D_i K^i}{K}$$

In doing so, we may rewrite EE (ZF) in

$$EE^{zf} = \frac{B(1 - \frac{(\tau^{(ul)} + \tau^{(dl)})K}{U}) \bar{R}}{\frac{B\sigma^2 \alpha S_x}{\eta} + C' + MD' + AB(1 - \frac{(\tau^{(ul)} + \tau^{(dl)})K}{U}) \bar{R}} \quad (4.18)$$

For given values of K and α the number of BS antennas maximizing the EE metric can be computed as [39];

$$M^{(o)} = \frac{e^w \left(\frac{\alpha \left(\frac{B\sigma^2 s_x}{\eta} \alpha + C' \right) + \frac{\alpha K - 1}{e}}{D'e} \right) + 1}{\alpha} + \alpha K - 1, \quad (4.19)$$

where $C' > 0$ and $D' > 0$

4.9 Optimal RF Power

Finding the EE-optimal total RF power the solution is given by following [39];

$$\alpha^* = \frac{e^w \left(\alpha \left(\frac{\eta}{B\sigma^2 s_x} \frac{(M - K)(C' + MD')}{e} - \frac{1}{e} \right) + 1 \right)}{M - K} - 1, \quad (4.20)$$

where $C' > 0$ and $D' >$

4.10 EE Optimization with Multi-cell Scenario

Consider the symmetric multi-cell scenario and concentrate on the cell in the middle. Each cell is a 500 x 500 square with uniformly distributed users, with the same minimum distance as in the single-cell scenario. We consider only interference that arrives from the two closest cells (in each direction). Motivated by the single-cell results, we consider only ZF processing and focus on comparing different pilot reuse patterns. The cells are divided into four clusters. Three different pilot reuse patterns are considered: the same pilots in all cells ($\tau^{(ul)} = 1$), two orthogonal sets of pilots with Cluster 1 and Cluster 4 having the same ($\tau^{(ul)} = 2$), and all clusters have different orthogonal pilots ($\tau^{(ul)} = 4$).

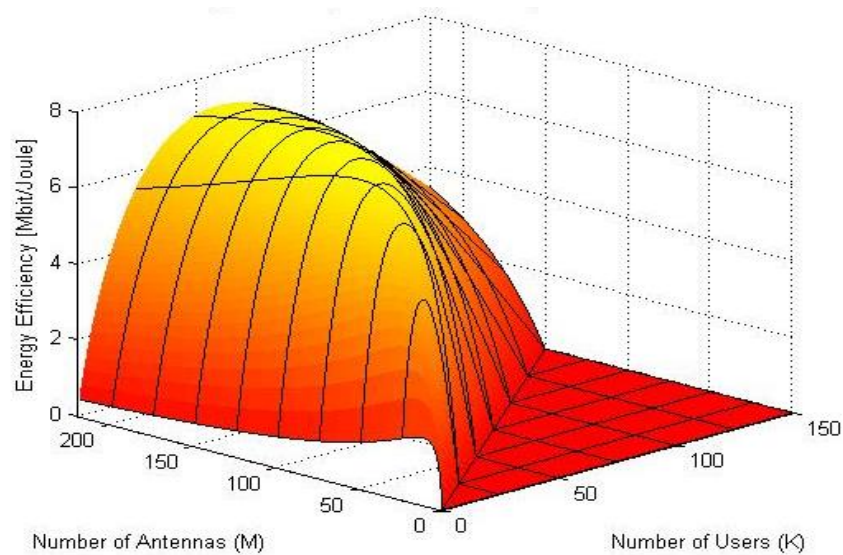


Figure 12: Energy efficiency (in Mbit/Joule) with ZF processing in the multi cell

Figure 12 shows the set of achievable EE values for different values of number of BS antennas M and users K . At pilot reuse of $\tau^{(ul)} = 4$ it is seen that EE has its highest value. This figure has smaller the optimal EE value since it occurs at the smaller system dimensions of $M = 123$ and $K = 40$. This is due to inter-cell interference, pilot overhead is

almost the same as in the single cell scenario, but the pilot reuse factor gives room for fewer user. It is clearly a massive MIMO setup and EE-optimal architecture is massive MIMO.

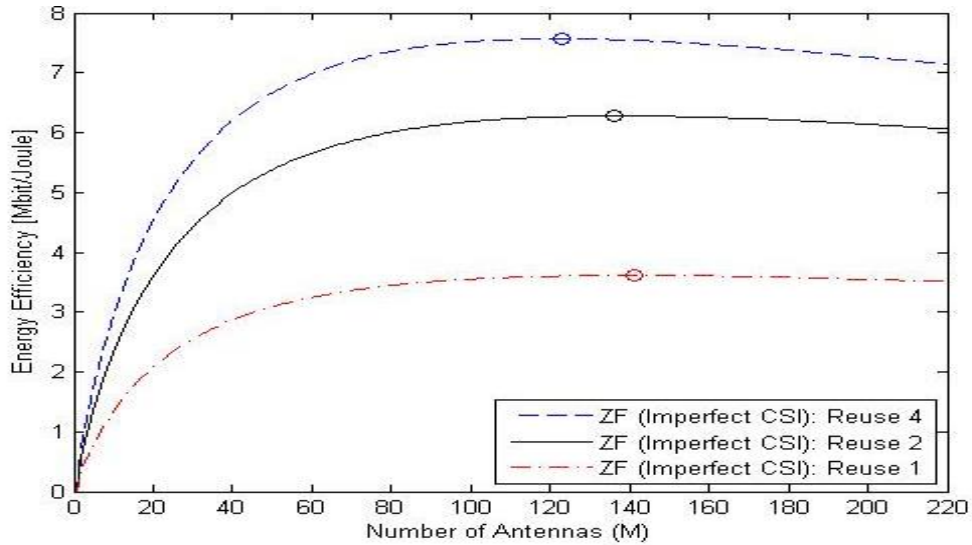


Figure 13: Maximal EE in the multi-cell scenario for different number of BS antennas and different pilot reuse factors.

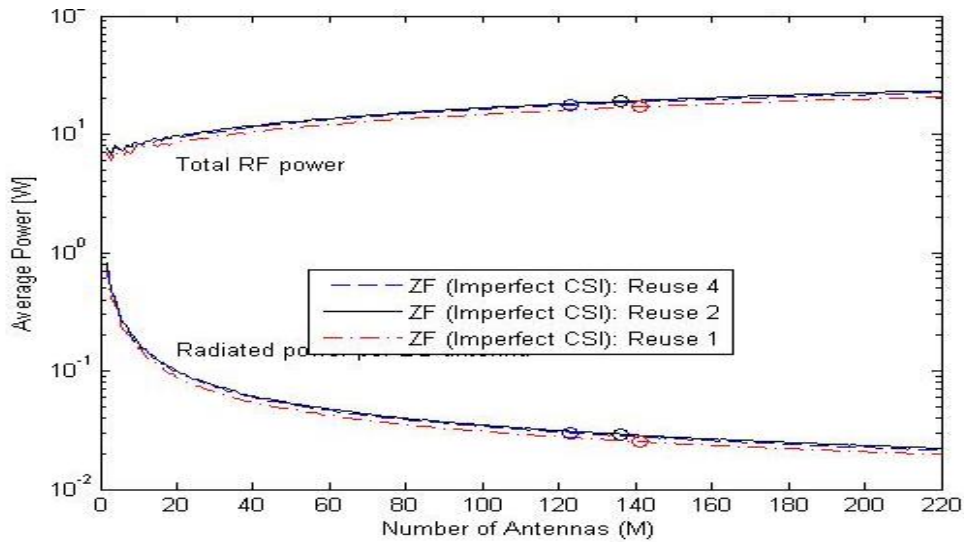


Figure 14: Total RF power at the EE-maximizing solution in the multi-cell scenario, for different number of BS antennas. The radiated power per BS antenna is also shown.

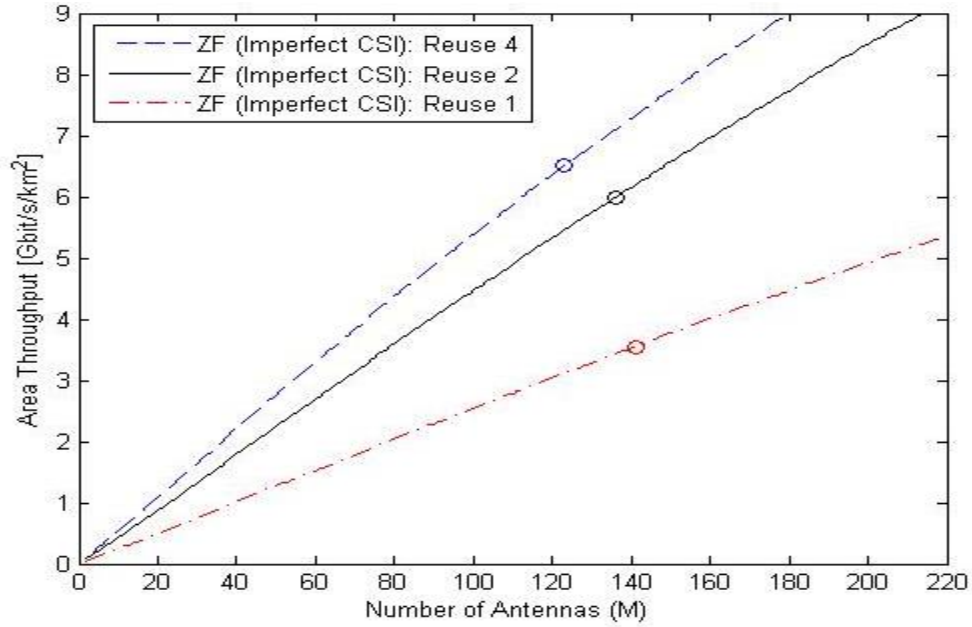


Figure 15: Area throughput at the EE-maximizing solution in the multi-cell scenario, for different number of BS antennas.

Figure 13 shows maximal EE for different number of antennas and figure 14 shows the corresponding RF power (and power per BS antenna) and figure 15 shows the corresponding area throughput for optimum EE values. Hence, the inter-cell interference affects the system by reducing the throughput, reducing the RF power consumption, and thereby also the EE. Interestingly, the largest pilot reuse factor ($\tau^{(ul)} = 4$) gives the highest EE and area throughput. This shows the necessity of actively mitigating pilot contamination in multi-cell systems. EE optimal increases by increasing transmit power but circuit power per BS antennas decreases with number of BS antennas.

Optimum EE in Massive MIMO using MMSE Precoding

5.1 Problem Statement

EE is equals the ratio between the average achievable sum information rate (in bit/channel use) and the total average power consumption (in Joule/channel use) and is measured in bit/Joule [8].

$$EE = \frac{\text{Average Sum Throughput} \left[\frac{\text{bit}}{\text{channel use}} \right]}{\text{Power Consumption} \left[\frac{\text{Joule}}{\text{channel use}} \right]}$$

EE metric for UL and DL takes the following form;

$$EE = \frac{\sum_{k=1}^K \{ (R_k^{ul}) + (R_k^{dl}) \}}{P_{TX}^{ul} + P_{TX}^{dl} + P_{CP}}, \quad (5.1)$$

where R_k^{ul} and R_k^{dl} are UL and DL rates of each user. P_{TX}^{ul}, P_{TX}^{dl} are uplink and downlink powers and P_{CP} accounts for the circuit power consumption.

It is required to design a detail model of circuit power consumption P_{CP} when dealing with the design of energy-efficient communication systems. An appropriate model for P_{CP} with

MMSE as a function of the three main design parameters, the number of BS antennas (M), number of active UEs (K), and the user gross rates (\bar{R}) is provided in detail.

5.2 Realistic Circuit Power Consumption Model

The total circuit power consumption P_{CP} is the sum of the power consumed by different analog components and digital signal processing [28]. Building on the prior works of [7], [28]–[32], a new refined circuit power consumption model for the multi-user MIMO system under investigation [10];

$$P_{CP}^{MMSE} = P_{FIX} + P_{TC} + P_{CE} + P_{C/D} + P_{BH} + P_{LP}^{MMSE}. \quad (5.2)$$

P_{FIX} is a constant quantity accounting for the fixed power consumption required for site-cooling, control signaling, and the load-independent power of backhaul infrastructure and baseband processors. P_{TC} accounts for the power consumption of the transceiver chains, P_{CE} of the channel estimation process (performed once per coherence block), $P_{C/D}$ of the channel coding and decoding units, P_{BH} of the load-dependent backhaul, and P_{LP} of the MMSE processing at the BS.

Now all these above mentioned power consumptions are discussed in detail.

a. Transceiver Chains. The power consumption P_{TC} of a set of typical transmitters and receivers can be quantified as;

$$P_{TC} = MP_{BS} + P_{SYN} + KP_{UE} \text{ Watt}, \quad (5.3)$$

where P_{BS} (as mentioned before) is the power required to run the circuit components (such as converters, mixers, and filters) attached to each antenna at the BS and P_{SYN} is the power consumed by the local oscillator. The last term P_{UE} accounts for the power required by all

circuit components (such as amplifiers, mixer, oscillator, and filters) of each single-antenna UE.

b. Channel Estimation. Let the computational efficiency be L_{BS} and L_{UE} arithmetic complex-valued operations per Joule (also known as flops/Watt) at the BS and UEs, respectively. There are $\frac{B}{U}$ coherence blocks per second and the pilot-based CSI estimation is performed once per block. In the uplink, the BS receives the pilot signal as $M \times \tau^{(ul)} K$ matrix and estimates each UE's channel by multiplying with the corresponding pilot sequence of length $\tau^{(ul)} K$. This is a standard linear algebra operation and requires

$$P_{CE}^{(ul)} = \frac{B}{U} \frac{2\tau^{(ul)} MK^2}{L_{BS}} \text{Watt}$$

In the downlink, each active UE receives a pilot sequence of length $\tau^{(dl)} K$ and processes it to acquire its effective pre-coded channel gain (one inner product) and the variance of interference plus noise (one inner product). We obtain

$$P_{CE}^{(dl)} = \frac{B}{U} \frac{2\tau^{(dl)} MK^2}{L_{US}} \text{Watt}$$

Therefore, the total power consumption $P_{CE} = P_{CE}^{(ul)} + P_{CE}^{(dl)}$ of the channel estimation process becomes [34];

$$P_{CE} = \frac{B}{U} \frac{2\tau^{(ul)} MK^2}{L_{BS}} + \frac{B}{U} \frac{4\tau^{(ul)} MK^2}{L_{UE}} \text{Watt}. \quad (5.4)$$

c. Coding and Decoding. In the downlink, the BS applies channel coding and modulation to K sequences of information symbols and each UE applies some suboptimal fixed-complexity algorithm for decoding its own sequence. The opposite is done in the uplink. The power consumption $P_{C/D}$ accounting for these processes is proportional to the number of bits and can thus be quantified as [10];

$$P_{C/D} = \sum_{k=1}^K (R_k^{(ul)} + R_k^{(dl)}) (P_{COD} + P_{DEC}) \text{Watt}, \quad (5.5)$$

where P_{COD} and P_{DEC} are the coding and decoding powers (in Watt per bit/s), respectively. For simplicity, we assume that P_{COD} and P_{DEC} are the same in the uplink and downlink, but it is straightforward to assign them different values.

d. **Backhaul.** The power consumption of the backhaul is commonly modeled as the sum of two parts. One load-independent and one load-dependent. The first part was already included in P_{FIX} , while the load-dependent part is proportional to the average sum rate. Looking jointly at the downlink and uplink, the load-dependent term P_{BH} can be computed as [10];

$$P_{C/D} = \sum_{k=1}^K (R_k^{(ul)} + R_k^{(dl)}), \quad (5.6)$$

where P_{BT} is the backhaul traffic power (in Watt per bit/second).

f. **Linear Processing.** The transmitted and received vectors of information symbols at the BS are generated by transmit precoding and processed by receive combining, respectively. This costs [10];

$$P_{LP} = B \left(1 - \frac{\tau^{(dl)} + \tau^{(ul)} K}{U} \right) \frac{2MK}{L_{BS}} + P_{LP-C}, \quad (5.7)$$

where the first term describes the power consumed by making one matrix-vector multiplication per channel use of data transmission. The second term P_{LP-C} , accounts for the power required for the computation of precoding and combining matrices \mathbf{G} and \mathbf{V} respectively [13];

$$\mathbf{G} = \begin{cases} \left(\begin{matrix} \mathbf{H} & \mathbf{P}^{ul} \mathbf{H}^H \\ \mathbf{H}^H & \mathbf{I}_M \end{matrix} + \sigma^2 \mathbf{I}_M \right)^{-1} \mathbf{H} \end{cases} \text{ for MMSE,} \quad (5.8)$$

and

$$\mathbf{V} = \begin{cases} \left(\begin{matrix} \mathbf{H} & \mathbf{P}^{ul} \mathbf{H}^H \\ \mathbf{H}^H & \mathbf{I}_M \end{matrix} + \sigma^2 \mathbf{I}_M \right)^{-1} \mathbf{H} \end{cases} \text{ for MMSE.} \quad (5.9)$$

The precoding and combining matrices are computed once per coherence block and the complexity depends strongly on the choice of processing scheme. Since $\mathbf{G} = \mathbf{V}$ is a natural choice (except when the uplink and downlink are designed very differently), we only need to compute one of them and thereby reduce the computational complexity. For MMSE processing using Cholesky factorization and back-substitution [34];

$$P_{LP-C}^{(MMSE)} = \frac{B}{U} \left(\frac{K^3}{L_{BS}} + \frac{9MK^2 + 3MK}{L_{BS}} \right), \quad (5.10)$$

computational cost is consumed.

By substituting all equations [(5.3)-(5.9)] in (5.2) and calculate the circuit power coefficient mentioned in the table below,

$C_0 = P_{FIX} + P_{SYN}$	$A = P_{COD} + P_{DEC} + P_{BT}$
$C_1 = P_{UE}$	$D_0 = P_{BS}$
$C_2 = \frac{4B\tau^{(dl)}}{UL_{UE}}$	$D_1 = \frac{B}{L_{BS}} \left(2 + \frac{9}{U} \right)$
$C_3 = \frac{B}{UL_{BS}}$	$D_2 = \frac{B}{UL_{BS}} (9 - 2\tau^{dl})$

Table 4 : Circuit Power Coefficient For MMSE Processing

For notational convenience, we introduce the constant coefficients A, $\{C_i\}$, and $\{D_i\}$ as reported in Table ;

$$P_{CP}^{MMSE} = \sum_{i=0}^3 C_i K_i + M \sum_{i=0}^2 D_i K_i + AK \left(1 - \frac{(\tau^{(ul)} + \tau^{(dl)}) K}{U}\right) \bar{R}. \quad (5.11)$$

In the following, we provide simple and realistic models for how each term in (5.2) depends, linearly or non-linearly, on the main system parameters M, K and α . This is achieved by characterizing the hardware setup using a variety of fixed coefficients, which are kept generic in the analysis; typical values are given in Table 5 [10];

Fixed power consumption (control signals, backhaul, etc.) P_{FIX}
Power consumed by local oscillator at BSs: P_{SYN}
Power required to run the circuit components at a BS: P_{BS}
Power required to run the circuit components at a UE: P_{UE}
Power required for coding of data signals: P_{COD}
Power required for decoding of data signals: P_{DEC}
Power required for backhaul traffic: P_{BT}

Table 5: Power consumption parameters values

5.3 Energy Efficiency Optimization with MMSE Processing

EE optimization is solved using for MMSE processing in the uplink and downlink. MMSE detector is employed with, we can without loss of generality parameterize the gross rate as:

$$\bar{R} = B \log(1 + \alpha(M - K)), \quad (5.12)$$

where α is a design parameter. Using this parameterization, the RF power required to guarantee each UE a gross rate of \bar{R} is [10];

$$P_{TX}^{ul-MMSE} = \frac{B\zeta^{ul}\sigma^2\alpha S_x}{\eta^{ul}} K, \quad (5.13)$$

where $S_x = \mathbb{E}\{(Lx)^{-1}\}$ accounts for user distribution and propagation environment. σ^2 denotes the noise variance (in Joule/channel use).

The average downlink RF power P_{TX}^{dl} required to serve each *UE* with a gross rate equal to \bar{R} then the average downlink RF power $P_{TX}^{dl-MMSE}$ required to serve each *UE* with a gross rate equal to \bar{R} is [10];

$$P_{TX}^{dl-MMSE} = \frac{B\zeta^{dl}\sigma^2\alpha S_x}{\eta^{dl}} K. \quad (5.14)$$

Average uplink and downlink RF powers with MMSE processing sum up to

$$P_{TX}^{MMSE} = P_{TX}^{ul-MMSE} + P_{TX}^{dl-MMSE} = \frac{B\sigma^2\alpha S_x}{\eta} K, \quad (5.15)$$

with

$$\eta = \left(\frac{\zeta^{ul}}{\eta^{ul}} + \frac{\zeta^{dl}}{\eta^{dl}} \right)^{-1}.$$

Now substituting (5.15) into (5.1)

$$EE^{MMSE} = \frac{K(1 - \frac{(\tau^{(ul)} + \tau^{(dl)})K}{U})\bar{R}}{\frac{B\sigma^2\alpha S_x}{\eta} K + P_{CP}^{MMSE}}, \quad (5.16)$$

where we used $R^{ul} + R^{dl} = (1 - \frac{(\tau^{(ul)} + \tau^{(dl)})K}{U})\bar{R}$ and since $\zeta^{ul} + \zeta^{dl} = 1$,

where $\bar{R} = B \log(1 + \alpha(M - K))$ and is also the function of (α, M, K) and yields

$$EE^{MMSE} = \frac{K(1 - \frac{(\tau^{(ul)} + \tau^{(dl)})K}{U})\bar{R}}{\frac{B\sigma^2\alpha S_x}{\eta}K + \sum_{i=0}^3 C_i K_i + M \sum_{i=0}^2 D_i K_i + AK(1 - \frac{(\tau^{(ul)} + \tau^{(dl)})K}{U})\bar{R}}. \quad (5.17)$$

In the following, we aim at solving (5.11) as a function of A , $\{C_i\}$ and $\{D_i\}$. In doing so, we first derive a closed-form expression for the EE-optimal value this bring indispensable insights on the interplay between these coefficients A , $\{C_i\}$ and $\{D_i\}$.

5.4 Simulation with MMSE Processing

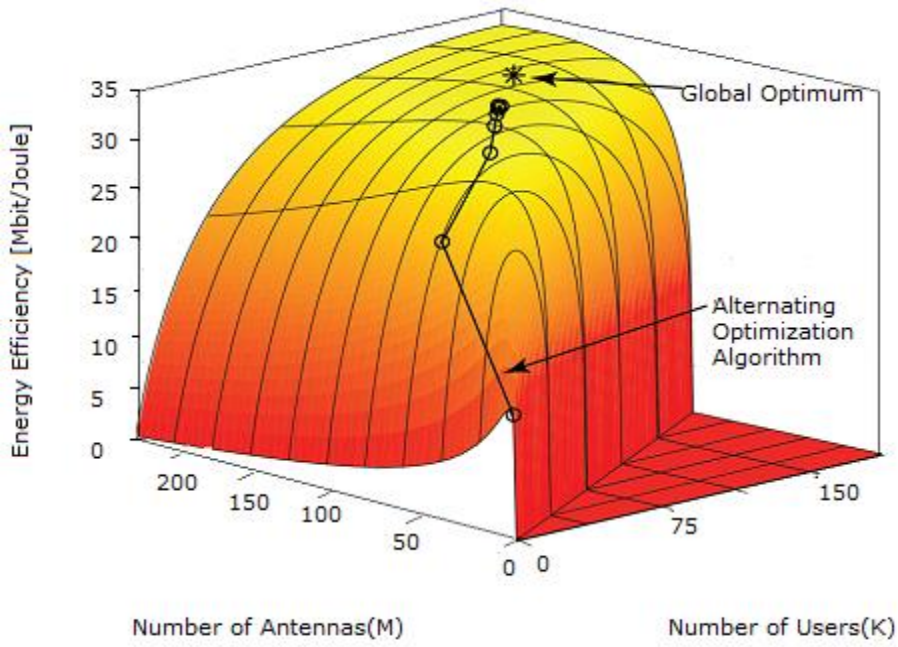


Figure 16: MMSE single cell scenario and perfect CSI

Figure 16 shows the set of achievable EE values with perfect CSI, MMSE processing, and for different values of M and K . The global optimum is marked with a star, while the convergence of the optimization algorithm is indicated with circles.

The global optimum is clearly a massive MIMO setup, which could be noted since it is the output of an optimization problem where we did not restrict the system dimensions whatsoever. In massive MIMO there is a tradeoff between power consumption and achievable rate and power consumption. EE is increase as increasing no. of transmit antennas while the power consumption also increases, which results the concave shape of EE curve. The surface in figure 16 is concave and quite smooth and we investigate an appropriate no. of BS antennas M and users K to maximize the EE. Thus, there is a variety of system parameters that provide close-to-optimal EE and the results appear to be robust to small changes in the circuit power coefficients. Although MMSE processing is optimal from a throughput perspective, we observe that MMSE processing achieves higher EE and has the (unnecessary) benefit of also handling $M < K$.

5.5 Comparison of MMSE with ZF and MRT Processing

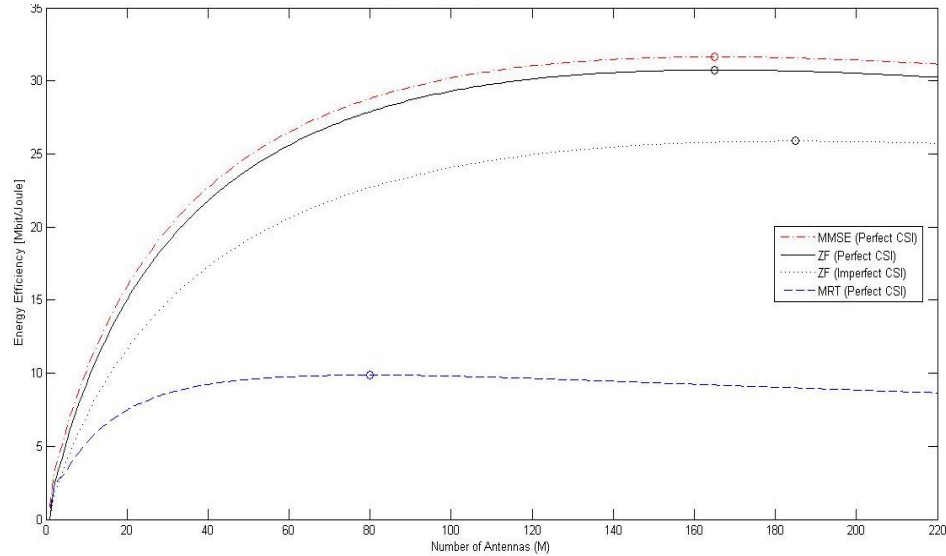


Figure 17: Maximal EE for different number of BS antennas and different processing schemes in the single-cell scenario.

To compare the different processing schemes, Figure 17 shows the maximum EE as a function of the number of BS antennas. Clearly, the similarity between MMSE and ZF shows an optimality of operating at high SNRs. ZF with imperfect CSI has a similar behavior as ZF and MMSE with perfect CSI. But MMSE perfect CSI is more EE than ZF because ZF cannot achieve good performance in practical scenarios such as under interference uncertainty and imperfect CSI.

We observe the behavior of curve that by increasing the no. of transmit antennas affect the tendency of EE critically. Increasing transmit antennas also increasing EE but if we consider large no. of transmit antennas the total circuit power consumption from analog

devices also increased but EE is less sensitive to power consumption in massive MIMO.

Curve after reaching its maximum EE will maintain its position.

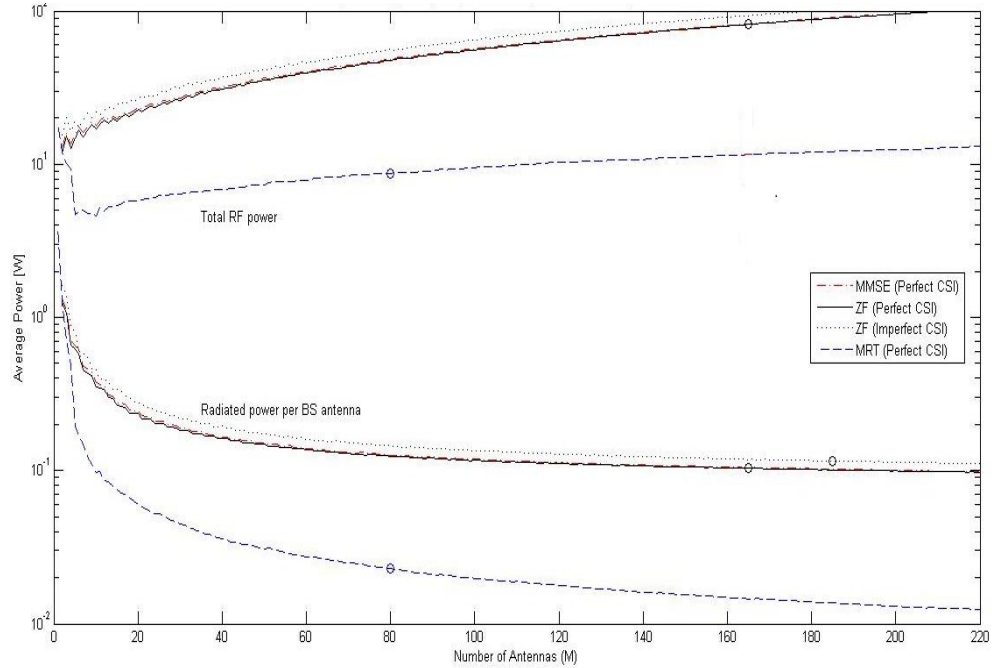


Figure 18: Total RF power at the EE-maximizing solution for different number of BS antennas in the single-cell scenario. The radiated power per BS antenna is also shown.

Next, Figure 18 shows the total RF power that maximizes the EE for different M (using the corresponding optimal K). For all the considered processing schemes, the most energy efficient strategy is to increase the RF power with M . Which indicated that the transmit power should be decreased with M . However, Figure 18 also shows that the transmit power per BS antenna decreases with M . The downlink transmit power with ZF and MMSE precoding is around 100 mW/antenna, while it drops to 23 mW/antenna with MRT. These numbers are much smaller than for conventional macro BSs (which operate at around 40×10^3 mW/antenna [33]) and reveals that the EE-optimal solution can be deployed with low-power UE-like RF amplifiers.

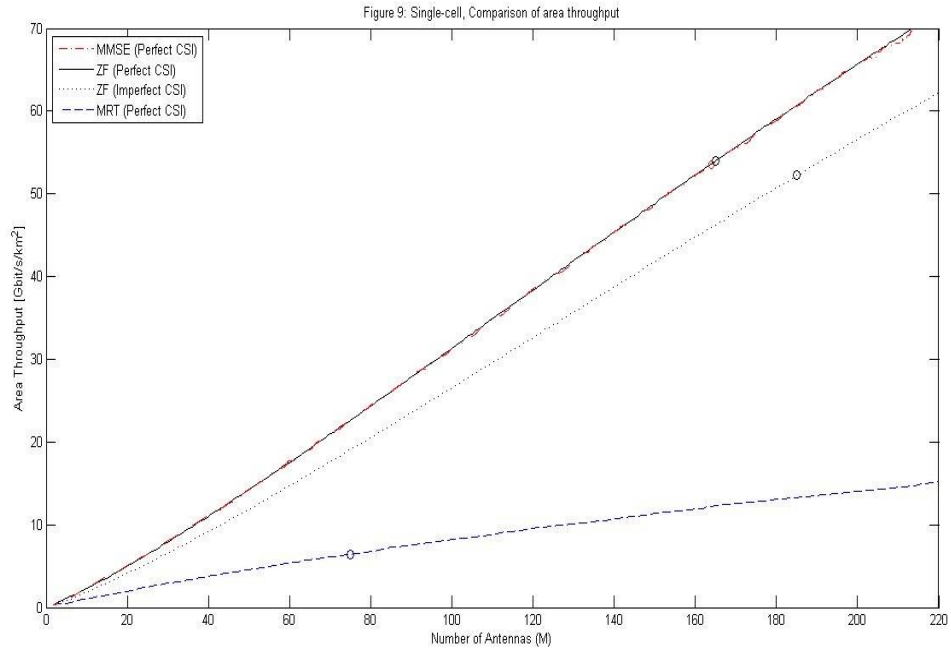


Figure 19: Area throughput at the EE-maximizing solution for different number of BS antennas in the single-cell scenario.

Figure 19 shows the area throughput (in Gbit/s/km²) that maximizes the EE for different M. Figure 19 shows that there is simultaneously an 8-fold improvement in area throughput. The majority of this gain is achieved also under imperfect CSI, which shows that massive MIMO with proper interference-suppressing precoding can achieve both great energy efficiency and unprecedented area throughput. In contrast, it is wasteful to deploy a large number of BS antennas and then co-process them using a MRT/MRC processing scheme that is severely limiting both the energy efficiency and area throughput.

Conclusions and Future Work

The presented work is come to an end in this chapter with further recommendations for future development based on the concepts presented here.

6.1 Conclusion

The presented thesis concludes many different useful interrelated concepts in regards to optimum energy efficiency. This thesis analyzed different sets of achievable EE for different transmit and receive antennas (i.e. K and M respectively) and gross rate R in energy efficient MU-MIMO systems. By using an architecture of power consumption at BS for today's communication networks, it describes all power consumption components in details especially power consumed for computational cost in linear processing and also analyzed its dependence on transmit and receive antennas. For numerical results closed form expressions are drive and analyze their behavior for the EE-maximizing. By considering Massive MIMO setup circuit power consumption increases but energy efficiency remains constant after reaching its maximum point so because of circuit power, energy efficiency is a quasi-concave function of transmitter and receiver thus it has a finite global optimum.

It is clear from numerical results that using Massive MIMO setup in today's circuitry, energy efficient optimal results are obtained and it is cleared that in the range of 10 – 100 mW Massive MIMO can use a low power equipment's (e.g., transmitter and

receiver antennas) instead of high power consumers equipment's. The results are quite stable to small changes in the circuit power coefficients.

6.2 Future Work

The presented thesis provides many pathways to innovatively improve the EE. The applicability in general MU-MIMO is an important open issue. This thesis has identified promising techniques for designing energy-efficient communication systems that can be optimized further. Since Massive MIMO is a new field, there can be several other ways to optimize EE using a combination of BS power consumption and power saving coordination for frequency reuse, power control and scheduling. All analyses in this work assumed a uniform distribution for users. It may also be relevant to explore distributions such as poisson process for this same scenario. This may have an effect particularly on the MU-Massive MIMO system.

References

- [1] E. Hossain, D. I. Kim, and V. K. Bhargava, *Cooperative Cellular Wireless Networks*, 1st ed. Cambridge University Press, 2011.
- [2] Q. Li, G. Li, W. Lee, M. il Lee, D. Mazzaresse, B. Clerckx, and Z. Li, "MIMO Techniques in WiMAX and LTE: A Feature Overview," *IEEE Commun. Mag.*, vol. 48, pp. 86–92, May 2010.
- [3] A. Maltsev, A. Khoryaev, A. Lomayev, R. Maslennikov, C. Antonopoulos, K. Avgeropoulos, A. Alexiou, F. Boccardi, Y. Hou, and K. Leung, "MIMO and Multihop Cross-Layer Design for Wireless Backhaul: A Testbed Implementation," *IEEE Commun. Mag.*, vol. 48, pp. 172–179, Mar. 2010.
- [4] K. Pahlavan and P. Krishnamurthy, "Principles of Wireless Networks; A Unified Approach", New Jersey: Prentice Hall, 2002.
- [5] [Cisco, 2013] Cisco (2013). <http://www.cisco.com/> Retrieved 18 April 2013.
- [6] Y. Chen, S. Zhang, S. Xu, and G. Li, "Fundamental trade-offs on green wireless networks," *IEEE Commun. Mag.*, vol. 49, no. 6, pp. 30–37, 2011.
- [7] H. Yang and T. Marzetta, "Total energy efficiency of cellular large scale antenna system multiple access mobile networks," in *Proc. IEEE Online Conference on Green Communications (OnlineGreenComm)*, 2013.
- [8] E. Björnson, J. Hoydis, M. Kountouris, and M. Debbah, "Massive MIMO systems with non-ideal hardware: Energy efficiency, estimation, and capacity limits," *IEEE Trans. Inf. Theory*, July 2013.

- [9] D. Ha, K. Lee, and J. Kang, "Energy efficiency analysis with circuit power consumption in massive MIMO systems," in Proc. IEEE Int. Symp. Personal, Indoor and Mobile Radio Commun. (PIMRC), 2013.
- [10] E. Björnson, L. Sanguinetti, J. Hoydis, M. Debbah, "Optimal Design of Energy-Efficient Multi-User MIMO Systems: Is Massive MIMO the Answer?," IEEE Trans. Wireless Communications, Mar2014.
- [11] G. Miao, "Energy-efficient uplink multi-user MIMO," IEEE Trans. Wireless Commun., vol. 12, no. 5, pp. 2302–2313, 2013.
- [12] E. Björnson, M. Kountouris, and M. Debbah, "Massive MIMO and small cells: Improving energy efficiency by optimal soft-cell coordination," in Proc. Int. Conf. Telecommun. (ICT), 2013
- [13] A Goldsmith, "Wireless Communications", published by Cambridge University press, 2012.
- [14] PRATHEEK UNNIKISHNAN ASWATH KUMAR R.DEEPA, Dr.K.BASKARAN. Study of spatial diversity schemes in multiple antenna systems. Theoretical and Applied Information Technology, 2005-2009:619{624, 2009.
- [15] RHODE and SCHWARZ. Introduction to mimo. Technical report, RHODE and SCHWARZ, 2009.
- [16] C Langton, Bernard Sklar, "Finding MIMO", October 2011, available online at http://complextoreal.com/tutorials/tutorial-27-finding-mimo/#.Uv-R_mSx1Y
- [17] A J Paulraj, D A Gore, R U Nabar, "An Overview of MIMO Communications—A Key to Gigabit Wireless", Published in the Proceedings of the IEEE, Vol. 92, No.2 February 2004.
- [18] M Simon and M S Alouini, 'performance of multichannel receivers' chapter 9 in "Digital Communication over Fading Channels A Unified Approach to Performance Analysis", published by Wiley, 2000, pp. 259-264.

- [19] E Biglieri, R Calderbank, A Constantinides, A Goldsmith, A Paulraj, H V Poor, "MIMO wireless Communication" published by Cambridge University Press 2007.
- [20] Q H Spencer, C B Peel, A L Swindle Hurst, M H Ilmenau, "An introduction to the Multi User MIMO Downlink", published in IEEE Communications Magazine 2004.
- [21] D Gesbert, M Kountouris, R W Heath Jr, Chan B Chae, T Slazar, "From Single User to Multiuser Communications; Shifting the MIMO Paradigm" published in IEEE Signal Processing Magazine 2007.
- [22] E G Larsson, F Tufvesson, O Edfors, T L Marzetta, "Massive MIMO for Next Generation Wireless Systems" IEEE Communications Magazine, Vol. 52, No. 2, pp. 186-195, Feb. 2014.
- [23] C Shepard, H Yu, N Anand, L Erran Li, T L Marzetta, R Yang, L Zhong, "Argos: Practical Many Antenna Base Stations", published in 'Mobicom 12' proceedings of the 18th annual international conference on Mobile Computing and Networking 2012, pages 53-64.
- [24] Lizhong Zheng and D. N. C. Tse, "Diversity and multiplexing: a fundamental tradeoff in multiple-antenna channels," Information Theory, IEEE Transactions on, vol. 49, pp. 1073-1096, 2003.
- [25] S. Cui, A. Goldsmith and A. Bahai, "Energy-efficiency of MIMO and cooperative MIMO techniques in sensor networks," IEEE J. Select. Areas Commun., vol. 22, pp. 1089, 2004.
- [26] F. Meywerk, The Mobile Broadband Vision-How to Make LTE a Success, LTE World Summit, London, UK, 2008.
- [27] Shor, Gadi. 2008. 'How Bluetooth, UWB, and 802.11 stack up on power consumption'.
- [28] G. Auer, O. Blume, V. Giannini, I. Godor, M. Imran, Energy efficiency analysis of the reference systems, areas of improvements and target breakdown. INFISO-ICT-247733 EARTH 2.0, 2012.

- [29] S. Tombaz, A. Vastberg, and J. Zander, "Energy- and cost-efficient ultrahigh- capacity wireless access," *IEEE Wireless Commun. Mag.*, vol. 18, no. 5, pp. 18–24, 2011.
- [30] S. Cui, A. Goldsmith, and A. Bahai, "Energy-efficiency of MIMO and cooperative MIMO techniques in sensor networks," *IEEE J. Sel. Areas Commun.*, vol. 22, no. 6, pp. 1089–1098, 2004.
- [31] A. Mezghani and J. A. Nossek, "Power efficiency in communication systems from a circuit perspective," in *Proc. IEEE Int. Symp. Circuits and Systems (ISCAS)*, 2011, pp. 1896–1899.
- [32] R. Kumar and J. Gurugubelli, "How green the LTE technology can be?" in *Proc. Wireless VITAE*, 2011.
- [33] Further advancements for E-UTRA physical layer aspects (Release 9). 3GPP TS 36.814, Mar. 2010.
- [34] S. Boyd and L. Vandenberghe, "Numerical linear algebra background."
- [35] D. Kang, D. Kim, Y. Cho, J. Kim, B. Park, C. Zhao, and B. Kim, "1.6–2.1 GHz broadband doherty power amplifiers for LTE handset applications," in *Proc. IEEE MTT-S Int. Microwave Symp. Digest*, 2011.
- [36] S. Tombaz, K. Sung, and J. Zander, "Impact of densification on energy efficiency in wireless access networks," in *Proc. IEEE Global Commun. Conf. (GLOBECOM)*, 2012.
- [37] M. Parker, "High-performance floating-point implementation using FPGAs," in *Proc. IEEE MILCOM*, 2009.
- [38] S. Boyd and L. Vandenberghe, *Convex Optimization*. Cambridge University Press, 2004.

- [39] T. Hungerford, *Abstract Algebra: An Introduction*. Brooks Cole, 1996.
- [40] F. Shmakov, “A universal method of solving quartic equations,” *Int. J. Pure and Applied Math.*, vol. 71, no. 2, pp. 251–259, 2011.
- [41] T. Marzetta, “Noncooperative cellular wireless with unlimited numbers of base station antennas,” *IEEE Trans. Wireless Commun.*, vol. 9, no. 11, pp. 3590–3600, 2010.